

1 Extending a land-surface model with *Sphagnum* moss to simulate responses  
2 of a northern temperate bog to whole-ecosystem warming and elevated CO<sub>2</sub>  
3

4 Xiaoying Shi<sup>1\*</sup>, Daniel M. Ricciuto<sup>1</sup>, Peter E. Thornton<sup>1</sup>, Xiaofeng Xu<sup>2</sup>, Fengming Yuan<sup>1</sup>,  
5 Richard J. Norby<sup>1</sup>, Anthony P. Walker<sup>1</sup>, Jeffrey Warren<sup>1</sup>, Jiafu Mao<sup>1</sup>, Paul J. Hanson<sup>1</sup>,  
6 Lin Meng<sup>3</sup>, David Weston<sup>1</sup>, Natalie A. Griffiths<sup>1</sup>

7 <sup>1</sup> Climate Change Science Institute and Environmental Sciences Division, Oak Ridge  
8 National Laboratory, Oak Ridge, TN 37831, USA

9 <sup>2</sup>Biology Department San Diego State University, San Diego, CA, 92182-4614, USA  
10

11 <sup>3</sup> Department of Geological and Atmospheric Sciences, Iowa State University, Ames, IA,  
12 50011  
13  
14

15 \* To whom correspondence should be addressed

16 Corresponding author's email: [shix@ornl.gov](mailto:shix@ornl.gov)

17 Fax: 865-574-2232  
18

19  
20  
21  
22  
23  
24  
25  
26  
27  
28  
29  
30  
31  
32  
33  
34  
35  
36  
37  
38  
39

40 **Abstract**

41  
42 Mosses need to be incorporated into Earth system models to better simulate  
43 peatland functional dynamics under changing environment. *Sphagnum* mosses are strong  
44 determinants of nutrient, carbon and water cycling in peatland ecosystems. However,  
45 most land surface models do not include *Sphagnum* or other mosses as represented plant  
46 functional types (PFTs), thereby limiting predictive assessment of peatland responses to  
47 environmental change. In this study, we introduce a moss PFT into the land model  
48 component (ELM) of the Energy Exascale Earth System Model (E3SM), by developing  
49 water content dynamics and non-vascular photosynthetic processes for moss. The model  
50 was parameterized and independently evaluated against observations from an  
51 ombrotrophic forested bog as part of the Spruce and Peatland Responses Under Changing  
52 Environments (SPRUCE) project. Inclusion of a *Sphagnum* PFT with some *Sphagnum*  
53 specific processes in ELM allows it to capture the observed seasonal dynamics of  
54 *Sphagnum* gross primary production (GPP), albeit with an underestimate of peak GPP.  
55 The model simulated a reasonable annual net primary production (NPP) for moss but  
56 with less interannual variation than observed, and reproduced above ground biomass for  
57 tree PFTs and stem biomass for shrubs. Different species showed highly variable  
58 warming responses under both ambient and elevated atmospheric CO<sub>2</sub> concentrations,  
59 and elevated CO<sub>2</sub> altered the warming response direction for the peatland ecosystem.  
60 Microtopography is critical: *Sphagnum* mosses on hummocks and hollows were  
61 simulated to show opposite warming responses (NPP decreasing with warming on  
62 hummocks, but increasing in hollows), and hummock *Sphagnum* was modeled to have  
63 strong dependence on water table height. Inclusion of this new moss PFT in global ELM

64 simulations may provide a useful foundation for the investigation of northern peatland  
65 carbon exchange, enhancing the predictive capacity of carbon dynamics across the  
66 regional and global scales.

## 67 **Copyright statement**

68 This manuscript has been authored by UT-Battelle, LLC under Contract No. DE-  
69 AC05-00OR22725 with the U.S. Department of Energy. The United States Government  
70 retains and the publisher, by accepting the article for publication, acknowledges that the  
71 United States Government retains a non-exclusive, paid-up, irrevocable, world-wide  
72 license to publish or reproduce the published form of this manuscript, or allow others to  
73 do so, for United States Government purposes. The Department of Energy will provide  
74 public access to these results of federally sponsored research in accordance with the DOE  
75 Public Access Plan (<http://energy.gov/downloads/doe-public-access-plan>).

## 76 77 **1. Introduction**

78  
79 Boreal peatlands store at least 500 Pg of soil carbon due to incomplete  
80 decomposition of plant litter inputs resulting from a combination of low temperature and  
81 water-saturated soils. Because of this capacity to store carbon, boreal peatlands have  
82 played a critical role in regulating the global climate since the onset of the Holocene  
83 (Frolking and Roulet, 2007; Yu et al., 2010). The total carbon stock is large but  
84 uncertain: a new estimation of northern peatlands carbon stock of 1055 Pg was recently  
85 reported by Nichols and Peteet (2019). The rapidly changing climate at high latitudes is  
86 likely to impact both primary production and decomposition rates in peatlands,  
87 contributing to uncertainty in whether peatlands will continue their function as net carbon

88 sinks in the long term (Moore et al., 1998; Turetsky et al., 2002; Wu and Roulet, 2014).  
89 Manipulative experiments and process-based models are thus needed to make defensible  
90 projections of net carbon balance of northern peatlands under anticipated global warming  
91 (Hanson et al, 2017; Shi et al., 2015).

92 Peatlands are characterized by a ground layer of bryophytes, and the raised or  
93 ombrotrophic bogs of the boreal zone are generally dominated by *Sphagnum* mosses that  
94 contribute significantly to total ecosystem CO<sub>2</sub> flux (Oechel and Van Cleve, 1986;  
95 Williams and Flanagan, 1998; Robroek et al., 2009; Vitt, 2014). *Sphagnum* mosses also  
96 strongly affect the hydrological and hydrochemical conditions at the raised bog surface  
97 (Van, 1995; Van der Schaaf, 2002). As a result, microclimate and *Sphagnum* species  
98 interactions influence the variability of both carbon accumulation rates and water and  
99 exchanges within peatland and between peatland and atmosphere (Heijmans et al., 2004a,  
100 2004b; Rosenzweig et al., 2008; Brown et al., 2010; Petrone et al., 2011; Goetz and Price,  
101 2015). Functioning as keystone species of boreal peatlands, *Sphagnum* mosses strongly  
102 influence the nutrient, carbon and water cycles of peatland ecosystems (Nilsson and  
103 Wardle, 2005; Cornelissen et al., 2007; Lindo and Gonzalez, 2010; Turetsky et al., 2010;  
104 Turetsky et al., 2012), and exert a substantial impact on ecosystem net carbon balance  
105 (Clymo and Hayward; 1982; Gorham, 1991; Wieder, 2006; Weston et el., 2015; Walker  
106 et al., 2017; Griffiths et al., 2018).

107 Numerical models are useful tools to identify knowledge gaps, examine long-term  
108 dynamics, and predict future changes. Earth system models (ESMs) simulate global  
109 processes, including the carbon cycle, and are primarily used to make future climate  
110 projections. Poor model representation of carbon processes in peatlands is identified as a

111 deficiency causing biases in simulated soil organic mass and heterotrophic respiratory  
112 fluxes for current ESMs (Todd-Brown et al., 2013; Tian et al., 2015). Although most  
113 ESMs do not include moss, a number of offline dynamic vegetation models and  
114 ecosystem models do include one or more moss plant functional types (PFTs) (Pastor et  
115 al., 2002; Nungesser, 2003; Zhuang et al., 2006; Bond-Lamberty et al., 2007; Heijmans et  
116 al., 2008; Euskirchen et al., 2009; Wania et al., 2009; Frohling et al., 2010). Several  
117 peatland-specific models contain moss species and have been applied globally or at  
118 selected peatland sites. For example, the McGill Wetland Model (MWM) was evaluated  
119 using the measurements at Degerö Stormyr and the Mer Bleue bogs (St-Hilaire et al.,  
120 2010). The peatland version of the General Ecosystem Simulator - Model of Raw Humus,  
121 Moder and Mull (GUESS-ROMUL) was used to simulate the changes of daily CO<sub>2</sub>  
122 exchange rates with water table position at a fen (Yurova et al., 2007). The PEATBOG  
123 model was implemented to characterize peatland carbon and nitrogen cycles in the Mer  
124 Bleue bog, including moss PFTs but without accounting for microtopography (Wu et al.,  
125 2013a). The CLASS-CTEM model (the coupled Canadian Land Surface Scheme and the  
126 Canadian Terrestrial Ecosystem Model), which includes a moss layer as the first soil  
127 layer, was applied to simulate water, energy and carbon fluxes at eight different peatland  
128 sites (Wu et al., 2016). The IAP-RAS (Institute of Applied Physics – Russian Academy  
129 of Sciences) wetland methane (CH<sub>4</sub>) model with a 10 cm thick moss layer (Mokhov et al.  
130 2007) was run globally to simulate the distribution of CH<sub>4</sub> fluxes (Wania et al., 2013).  
131 The CHANGE model (a coupled hydrological and biogeochemical process simulator),  
132 which includes a moss cover layer (Launiainen et al., 2015), was used to investigate the  
133 effect of moss on soil temperature and carbon flux at a tundra site in Northeastern Siberia

134 (Park et al., 2018). Chadburn et al. (2015) added a surface layer of moss to JULES land  
135 surface model to consider the insulating effects and treated the thermal conductivity of  
136 moss depending on its water content to investigate the permafrost dynamics. Porada et al.  
137 (2016) integrated a stand-alone dynamic non-vascular vegetation model LiBry (Porada et  
138 al., 2013) to land surface scheme JSBACH, but JSBACH mainly represent bryophyte and  
139 lichen cover on upland forest, not for peatland ecosystem. Druel et al. (2017) investigated  
140 the vegetation-climate feedbacks in high latitudes by introducing a non-vascular plant  
141 type representing mosses and lichens to the global land surface model ORCHIDEE.  
142 Moreover, those models did not consider microtopography and the lateral transports  
143 between hummocks and hollows. Two models, the “ecosys” model (Grant et al., 2012)  
144 and CLM\_SPRUCE (Shi et al., 2015), have been parameterized to represent peatland  
145 microtopographic variability (e.g., the hummock and hollow microterrain characteristic  
146 of raised bogs) with lateral connections across the topography. Prediction of water table  
147 dynamics in the “ecosys” model is constrained by specifying a regional water table at a  
148 fixed height and a fixed distance from the site of interest, thereby missing key controlling  
149 factors of a precipitation-driven dynamic water table (Shi et al., 2015). The  
150 CLM\_SPRUCE model (Shi et al., 2015) was developed to parameterize the hydrological  
151 dynamics of lateral transport for microtopography of hummocks and hollows in the raised  
152 bog environment of the SPRUCE (Spruce and Peatland Responses Under Changing  
153 Environments) experiment (Hanson et al., 2017). That model version did not include the  
154 biophysical dynamics of *Sphagnum* moss, and used a prescribed leaf area instead of  
155 allowing leaf area to evolve prognostically.

156 In this study, we introduce a new *Sphagnum* moss PFT into the model, and migrate  
157 the entire raised-bog capability into the new Energy Exascale Earth System Model  
158 (E3SM), specifically into version 1 of the E3SM land model (ELM v1, Ricciuto et al.,  
159 2018). The objectives of this study are to: 1) introduce a *Sphagnum* PFT to the ELM  
160 model with additional *Sphagnum*-specific processes to better capture the peatland  
161 ecosystem; and 2) apply the updated ELM to explore how an ombrotrophic, raised-dome  
162 bog peatland ecosystem will respond to different scenarios of warming and elevated  
163 atmospheric CO<sub>2</sub> concentration.

## 164 **2. Model description**

### 165 **2.1 Model provenance**

166 ELM v1 is the land component of E3SM v1, which is supported by the US  
167 Department of Energy (DOE). Developed by multiple DOE laboratories, E3SM consists  
168 of atmosphere, land, ocean, sea ice, and land ice components, linked through a coupler  
169 that facilitates across-component communication (Golaz et al., 2019). ELM was  
170 originally branched from the Community Land Model (CLM4.5, Oleson et al., 2013),  
171 with new developments that include representation of coupled carbon, nitrogen, and  
172 phosphorus controls on soil and vegetation processes, and new plant carbon and nutrient  
173 storage pools (Ricciuto et al., 2018; Yang et al., 2019; Burrows et al., 2020). Inputs of  
174 new mineral nitrogen of ELM are from atmospheric deposition and biological nitrogen  
175 fixation. The fixation of new reactive nitrogen from atmospheric N<sub>2</sub> by soil  
176 microorganisms is an important component of nitrogen budgets. ELM follows the  
177 approach of Cleveland et al. (1999) that uses an empirical relationship of biological

178 nitrogen fixation as a function of net primary production to predict the nitrogen fixation.  
179 The model version used in this study is designated ELM\_SPRUCE, and includes the new  
180 implementation of *Sphagnum* mosses as well as the hydrological dynamics of lateral  
181 transport between hummock and hollow microtopographies. The implementation has  
182 been parameterized based on observations from the S1-Bog in northern Minnesota, USA,  
183 as described by Shi et al. (2015), with additional details provided below.

## 184 2.2 Non-vascular plants: *Sphagnum* mosses

185 To represent non-vascular plant the *Sphagnum* mosses, we modified the C3 artic  
186 grasses equations as follows. We considered *Sphagnum* biomass to be represented mainly  
187 by leaf and stem carbon (only a very shallow root). In addition, we modified the vascular  
188 C3 arctic grasses equations for photosynthesis and stomatal conductance (see the below  
189 new model development), and the associated parameters as reported by Table 1-3. We  
190 use the same framework as for C3 arctic grasses, but the Ball-Berry slope term is assumed  
191 to be zero and the intercept term is the conductance term as a function of water content of  
192 *Sphagnum* mosses. For all other processes like the evapo(transpi)ration and associated  
193 parameters not described below, we used the C3 arctic grasses equations (reported by  
194 Oleson et al., 2013). Drying impacts the conductance and affects evapo(transpi)ration of  
195 the internal water. The specific leaf area (SLA) and leaf C:N ratio parameters are strong  
196 controls on the maximum rate of Rubisco carboxylase activity ( $V_{cmax}$ ), and therefore  
197 overall productivity and *Sphagnum* moss leaf area index (LAI). The high sensitivities  
198 occur because LAI is a strong control on evapo(transp)iration.

## 199 **2.3 New model developments**

### 200 **2.3.1 Water content dynamics of *Sphagnum* mosses**



201 The main sources for water content of *Sphagnum* mosses are passive capillary  
202 water uptake from peat, and interception of atmospheric water on the capitulum (growing  
203 tip of the moss) (Robroek et al. 2007). Capillary water uptake, the internal *Sphagnum*  
204 moss water content, is modeled as functions of soil water content and evaporation losses.  
205 Water intercepted on the *Sphagnum* moss capitulum is modeled as a function of moss  
206 foliar biomass, current canopy water, water drip, and evaporation losses.

207 Since evaporation at the *Sphagnum* surface depends on atmospheric water vapor  
208 deficit, moss-atmosphere conductance and available water pool which depends on  
209 capillary wicking of water up to the surface. we developed a relationship between  
210 measured soil water content at depth and surface *Sphagnum* water content. At SPRUCE,  
211 the peat volumetric water content is measured at several depths using automated sensors  
212 (model 10HS, Decagon Devices, Inc., Pullman, WA) calibrated for the site-specific upper  
213 peat soil using mesocosms (reference Figure S1, Hanson et al. 2017). During those  
214 calibrations, we periodically sampled the surface *Sphagnum* for gravimetric water content  
215 and water potential using a dew point potentiometer (WP4, Decagon Devices, Inc.),  
216 which also provided a surface soil water retention curve. The destructive sampling of  
217 surface *Sphagnum* was primarily hummock species but did included some hollow  
218 species. The automated measurements of peat water content at 10 cm depth were shown  
219 to be a good indicator of surface *Sphagnum* water content (Fig. 1). Based on this  
220 relationship, we model the water content of *Sphagnum* moss due to capillary rise  
221 ( $W_{internal}$ ) (g water /g dry moss) as:

$$222 \quad W_{internal} = 0.3933 + 7.6227 / (1 + \exp(-(Soil_{vol} - 0.1571)) / 0.018) \quad (1)$$

223 where  $Soil_{vol}$  is the averaged volumetric soil water of modeled soil layers nearest the

224 10cm depth horizon (layers 3 and 4 in the ELM v1 vertical layering scheme).

225 The *Sphagnum* moss surface water ( $W_{surface}$ ) was calculated using the model

226 predicted canopy water and the dry foliar biomass as:

$$227 \quad W_{surface} = can\_water / fmass \quad (2)$$

228 where  $W_{surface}$  (g water /g dry moss) is the surface water content and  $fmass$  is the foliar

229 biomass of *Sphagnum* mosses. The  $can\_water$  is the *Sphagnum* moss canopy water and it

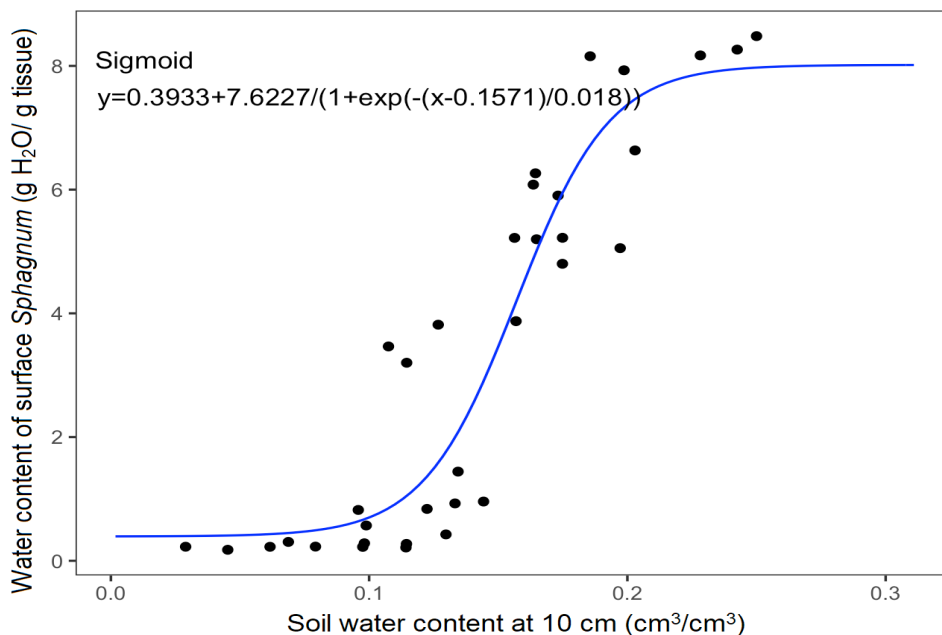
230 is simulated by a function of interception, canopy drip, dew and canopy evaporation

231 (Oleson et al., 2013).

232 The total water content ( $W_{total}$ ) of *Sphagnum* mosses is the sum of water taken

233 up from peat and the surface water content (St-Hilaire et al, 2010; Wu et al., 2013).

$$234 \quad W_{total} = W_{internal} + W_{surface} \quad (3)$$



235

236

237 Figure 1. The measured relationship between soil water content at depth and the water content of  
238 surface *Sphagnum* based on destructive sampling.

239

### 240 **2.3.2 Modeling *Sphagnum* CO<sub>2</sub> conductance and photosynthesis**

241 ELM\_SPRUCE computes photosynthetic carbon uptake (gross primary  
242 production, or GPP) for each vascular PFT on a half-hourly time step, based on the  
243 Farquhar biochemical approach (Farquhar et al., 1980; Collatz et al., 1991, 1992), with  
244 implementation as described by Oleson et al. (2013). While, *Sphagnum* lacks a leaf  
245 cuticle and stomata that regulate water loss and CO<sub>2</sub> uptake in vascular plants (Titus et al.  
246 1983). The primary transport pathway for CO<sub>2</sub> is through the cells and is analogous to  
247 mesophyll conductance in higher plants. Thus, we calculate the total conductance to CO<sub>2</sub>  
248 for *Sphagnum* mosses by using total water content following the method reported by  
249 Williams and Flanagan (1998) described as below. Goetz and Price (2015) also indicated  
250 that capillary rise through the peat is essential to maintain a water content sufficient for  
251 photosynthesis for *Sphagnum* moss species, but that atmospheric inputs can provide small  
252 but critical amounts of water for physiological processes.

253 The stomatal conductance for vascular plant types in ELM\_SPRUCE is derived  
254 from the Ball-Berry conductance model (Collatz et al., 1991). That model relates  
255 stomatal conductance to net leaf photosynthesis, scaled by the relative humidity and the  
256 CO<sub>2</sub> concentration at the leaf surface. The stomatal conductance ( $g_s$ ) and boundary layer  
257 conductance ( $g_b$ ) are required to obtain the internal leaf CO<sub>2</sub> partial pressure ( $C_i$ ) of  
258 vascular PFTs:

$$259 \quad C_i = C_a - \left( \frac{1.4g_s + 1.6g_b}{g_s g_b} \right) P_{atm} A_n \quad (4)$$

260 where  $C_i$  is the internal leaf CO<sub>2</sub> partial pressure,  $C_a$  is the atmospheric CO<sub>2</sub> partial  
 261 pressure,  $A_n$  is leaf net photosynthesis ( $\mu$  mol CO<sub>2</sub> m<sup>-2</sup> s<sup>-1</sup>)  $P_{atm}$  is the atmospheric  
 262 pressure, and values 1.4 and 1.6 are the ratios of the diffusivity of CO<sub>2</sub> to H<sub>2</sub>O for  
 263 stomatal conductance and the leaf boundary layer conductance, respectively.

264 For *Sphagnum* moss photosynthesis, we followed the method from the McGill  
 265 Wetland Model (St-Hilaire et al. 2010; Wu et al., 2013), which is based on the effects of  
 266 *Sphagnum* moss water content on photosynthetic capacity (Tenhunen et al., 1976) and  
 267 total conductance of CO<sub>2</sub> (Williams and Flanagan, 1998), and replaces the stomatal  
 268 conductance representation used for vascular PFTs.

$$269 \quad C_i = C_a - \frac{P_{atm}A_n}{g_{tc}} \quad (5)$$

270 The total conductance to CO<sub>2</sub> ( $g_{tc}$ ) was determined from a least-squares regression  
 271 described by Williams and Flanagan (1998) as:

$$272 \quad g_{tc} = -0.195 + 0.134W_{total} - 0.0256W_{total}^2 + 0.0028W_{total}^3 - \\ 273 \quad 0.0000984W_{total}^4 + 0.00000168W_{total}^5 \quad (6)$$

274 where  $W_{total}$  is as defined in equation (3). This relationship is only valid up to the  
 275 maximum water holding capacity of mosses. To be noted that we assume that the  
 276 boundary layer conductance is greater than moss surface layer conductance, and the moss  
 277 surface layer conductance is greater than chloroplast conductance.

278 In addition to the water content, the effects of moss submergence were taken into  
 279 account in the calculation of moss photosynthesis. Walker et al. (2017) reported

280 significant impacts of submergence on measured *Sphagnum* GPP and modeled the effect  
281 by modifying the *Sphagnum* leaf (stem) area index. Submergence in Walker et al. (2017)  
282 was expressed as photosynthesising stem area index (SAI) as a logistic function of water  
283 table depth. A maximum SAI of 3 was used and the parameter combination that most  
284 closely described the GPP data gave a range of water table depth from -10 cm for  
285 complete submergence and SAI of ~2.5 at 10 cm. This allowed for a range of processes  
286 such as floatation of *Sphagnum* with the water table, and adhesion of water to the  
287 *Sphagnum* capitula. For simplicity, in ELM\_SPRUCE, we calculated such impacts on  
288 *Sphagnum* GPP directly as a function of the height of simulated surface water, assuming  
289 that GPP from the submerged portion of photosynthetic tissue is negligible. GPP is thus  
290 reduced linearly according to the following equation:

$$291 \quad GPP_{\text{sub}} = GPP_{\text{orig}} * (h_{\text{moss}} - H_2O_{\text{sfc}}) \quad (7)$$

292 where  $GPP_{\text{sub}}$  is the GPP corrected for submergence effects,  $GPP_{\text{orig}}$  is the original GPP,  
293  $H_2O_{\text{sfc}}$  is the surface water height, and  $h_{\text{moss}}$  is the height of the photosynthesizing  
294 *Sphagnum* layer above the soil surface, set to 5cm in our simulations. If  $H_2O_{\text{sfc}}$  is equal to  
295 or greater than  $h_{\text{moss}}$ , GPP is reduced to zero. Because in our simulations surface water is  
296 never predicted to occur in the hummocks, in practice this submergence effect only  
297 affects the moss GPP in the hollows.

### 298 **3. Methods**

#### 299 **3.1 Site Description**

300 We focused on a high C, ombrotrophic peatland (the S1-Bog) that has a perched  
301 water table with limited groundwater influence (Sebestyen et al. 2011, Griffiths and

302 Sebestyen, 2016). This southern boreal bog is located on the Marcell Experimental  
303 Forest, approximately 40 km north of Grand Rapids, Minnesota, USA (47.50283 degrees  
304 latitude, -93.48283 degrees longitude) (Sebestyen et al. 2011), and is the site of the  
305 SPRUCE climate change experiment (<http://mnspruce.ornl.gov>; Hanson et al., 2017). The  
306 S1-Bog has a raised hummock and sunken hollow microtopography, and it is nearly  
307 covered by *Sphagnum* mosses. *S. angustifolium* (C.E.O. Jensen ex Russow) and *S. fallax*  
308 (Klinggr.) occupy 68% of the moss layer and exist in both hummocks and hollows. *S.*  
309 *magellenicum* (Brid.) occupies ~20% of the moss layer and is primarily limited to the  
310 hummocks (Norby et al., 2019). The vascular plant community at the S1-Bog is  
311 dominated by the evergreen tree *Picea mariana* (Mill.) B.S.P, the deciduous tree *Larix*  
312 *laricina* (Du Roi) K. Koch, and a variety of ericaceous shrubs. Trees are present due to  
313 natural regeneration following strip cut harvesting in 1969 and 1974 (Sebestyen et al.,  
314 2011). The soil of this peat bog is the Greenwood series, a Typic Haplohemist  
315 (<https://websoilsurvey.sc.egov.usda.gov>), and its average peat depth is 2 to 3 m  
316 (Parsekian et al., 2012)

317 Northern Minnesota has a subhumid continental climate with average annual  
318 precipitation of 768 mm and annual air temperature of 3.3 °C for the time period from  
319 1965 to 2005. Mean annual air temperatures at the bog have increased about 0.4 °C per  
320 decade over the last 40 years (Verry et al., 2011).

### 321 **3.2 Field measurements**

322 Multiple observational pre-treatment data (the data were collected prior to  
323 initiation of the warming and CO<sub>2</sub> treatments) were used in this study. Flux-partitioned  
324 GPP of *Sphagnum* mosses was derived from measured hourly *Sphagnum*-peat net

325 ecosystem exchange (NEE) flux (Walker et al., 2017). The GPP – NEE relationship was  
326 also evaluated using observed vegetation growth and productivity allometric and biomass  
327 data on tree species, stem biomass for shrub species (Hanson et al., 2018a and b), and  
328 *Sphagnum* pre-treatment net primary productivity (NPP) (Norby et al., 2019).  
329 ELM\_SPRUCE was driven by climate data (temperature, precipitation, relative humidity,  
330 solar radiation, wind speed, pressure and long wave radiation) from 2011 to 2017  
331 measured at the SPRUCE S1-Bog (Hanson et al., 2015a and b). The surface weather  
332 station is outside of the enclosures and not impacted by the experimental warming  
333 treatments that began in 2015. These data are available at <https://mnspruce.ornl.gov/>.

334

### 335 **3.3 Simulation of the SPRUCE experiment**

336       Based on measurements at the SPRUCE site, ELM\_SPRUCE includes four  
337 PFTs: boreal evergreen needleleaf tree (*Picea*), boreal deciduous needleleaf tree (*Larix*),  
338 boreal deciduous shrub (representing several shrub species), and the newly introduced  
339 *Sphagnum* moss PFT. Currently ELM\_SPRUCE does not include light competition  
340 among multiple PFTs, and thus does not represent cross-PFT shading effects. Our model  
341 also allows the canopy density of PFTs to change prognostically, and their fractional  
342 coverage is held constant. We used measurements from *Sphagnum* moss collected at a  
343 tussock tundra site in Alaska (Hobbie 1996) to set several of the model leaf litter  
344 parameters for our simulations (Table 1). The values for other parameters have been  
345 optimized based on observations at the SPRUCE site (Table 2 and 3, optimization  
346 methods described in section 3.4). We prescribe both hummock and hollow  
347 microtopographies to have the same fractional PFT distribution. Consistent with Shi et

348 al. (2015), hummocks and hollows were modeled on separate columns with lateral flow  
349 of water between them. All the ELM\_SPRUCE simulations were conducted using a  
350 prognostic scheme for canopy phenology (Olesen et al., 2013).

351 The SPRUCE experiment at the S1-Bog consists of combined manipulations of  
352 temperature (various differentials up to +9 °C above ambient) and atmospheric CO<sub>2</sub>  
353 concentration (ambient and ambient + 500 ppm) applied in 12 m diameter x 8 m tall  
354 enclosures constructed in the S1-Bog. The whole-ecosystem warming began in August  
355 2015, elevated CO<sub>2</sub> started from June 2016, and various treatments are envisioned to  
356 continue until 2025. Extensive pre-treatment observations at the site began in 2009.

357 For the ELM\_SPRUCE, we continuously cycled the 2011-2017 climate forcing  
358 (see section 3.2) to equilibrate carbon and nitrogen pools under pre-industrial  
359 atmospheric CO<sub>2</sub> concentrations and nitrogen deposition, and then launched a simulation  
360 starting from year 1850 through year 2017. This transient simulation includes historically  
361 varying CO<sub>2</sub> concentrations, nitrogen deposition, and the land-use effects of a strip cut  
362 and harvest at the site in 1974. These simulations were used to compare model  
363 performance with pre-treatment observations. A subset of these observations was also  
364 used for optimization and calibration (section 3.4).

365 To investigate how the bog vegetation may respond to different warming  
366 scenarios and elevated atmospheric CO<sub>2</sub> concentrations, we performed 11 model runs  
367 from the same starting point in year 2015. These simulations were designed to reflect the  
368 warming treatments and CO<sub>2</sub> concentrations being implemented in the SPRUCE  
369 experiment enclosures. The model simulations include one ambient case (both ambient  
370 temperature and CO<sub>2</sub> concentration), and five simulations with modified input air



371 temperatures to represent the whole-ecosystem warming treatments at five levels (+0 °C,  
 372 +2.25 °C, +4.50 °C, +6.75 °C and +9.00 °C above ambient) and at ambient CO<sub>2</sub>, and  
 373 another five simulations with the same increasing temperature levels and at elevated CO<sub>2</sub>  
 374 (900 ppm). In the treatment simulations, we also considered the passive enclosure  
 375 effects, which reduce incoming shortwave and increase incoming longwave radiation  
 376 (Hanson et al., 2017). Following the SPRUCE experimental design, there was no water  
 377 vapor added so that the simulations used constant specific humidity instead of constant  
 378 relative humidity across the warming levels. All the treatment simulations were  
 379 performed through the year 2025 by continuing to cycle the 2011-2017 meteorological  
 380 inputs (with modified temperature and radiation to reflect the treatments) to simulate  
 381 future years.

382 Table 1: Physiological parameters of *Sphagnum* mosses as given in Hobbie 1996

Parameters	Description	Values
lflitcn	Leaf litter C:N ratio (gC/gN)	66
lf_fcel	Leaf litter fraction of cellulose	0.737
lf_flab	Leaf litter fraction of labile	0.227
lf_flg	Leaf litter fraction of lignin	0.036

383

### 384 **3.4. Model sensitivity analysis and calibration**

385 The vegetation physiology parameters in ELM\_SPRUCE were originally derived  
 386 from CLM4.5 and its predecessor, Biome-BGC, and represent broad aggregations of  
 387 plant traits over many species and varied environmental conditions (White et al., 2000).

388 To achieve reasonable model performance at SPRUCE, site-specific parameters and  
389 targeted parameter calibration are needed. Since the ELM\_SPRUCE contains over 100  
390 uncertain parameters, parameter optimization is not computationally feasible without first  
391 performing some dimensionality reduction. Based on previous ELM sensitivity analyses  
392 (e.g., Lu et al., 2018; Ricciuto et al., 2018; Griffiths et al., 2018), we chose 35 model  
393 parameters for further calibration (Tables 2 and 3). An ensemble of 3000 ELM\_SPRUCE  
394 simulations were conducted using the procedure described in 3.3, with each ensemble  
395 member using a randomly selected set of parameter values within uniform prior ranges.  
396 This model ensemble was first used to construct a polynomial chaos surrogate model,  
397 which was then used to perform a global sensitivity analysis (Sargsyan et al., 2014;  
398 Ricciuto et al., 2018). Main sensitivity indices, reflecting the proportion of output  
399 variance that occurs for each parameter, are described in section 4.1.

400 To minimize potential biases in model predictions of treatment responses, we  
401 calibrated the same 35 model parameters using pre-treatment observations as data  
402 constraints. We employed a quantum particle swarm optimization (QPSO) algorithm (Lu  
403 et al., 2018). While this method does not allow for the calculation of posterior prediction  
404 uncertainties, it is much more computationally efficient than other methods such as  
405 Markov Chain Monte Carlo. The constraining data included year 2012-2013 tree growth  
406 and biomass (Hanson et al. 2018a), year 2012-2013 shrub growth and biomass (Hanson  
407 et al., 2018b), year 2012 and 2014 *Sphagnum* net primary productivity (Norby et al.,  
408 2017, 2019), enclosure-averaged leaf area index by PFT (year 2011 for tree and year  
409 2012 for shrub and *Sphagnum*), and year 2011-2013 water table depth (WTD)  
410 observations, aggregated to seasonal averages (Hanson et al., 2015b). The goal of the

411 optimization is to minimize a cost function, which we define here as a sum of squared  
 412 errors over all observation types weighted by observation uncertainties. When  
 413 observation uncertainties were not available, we assumed a range of  $\pm 25\%$  from the  
 414 default value. Site measurements were also used to constrain the ranges of two  
 415 parameters: *leafcn* (leaf carbon to nitrogen ratio) and *slatop* (specific leaf area at canopy  
 416 top). The uniform prior ranges for these parameters represent the range of plot to plot  
 417 variability. Optimized parameter values are shown in Table 2 and 3. Section 4 reports the  
 418 results of simulations using these optimized parameters, which were used to perform a  
 419 spinup, transient (1850-2017) and set of 11 treatment simulations (2015-2025) as  
 420 described above.

421 Table 2: PFT-specific optimized model parameters

Parameter	Description	<i>Sphagnum</i>	<i>Picea</i>	<i>Larix</i>	Shrub	Range
flnr	Rubisco-N fraction of leaf N	0.2906	0.0678	0.2349	0.2123	[0.05,0.30]
croot_stem	Coarse root to stem allocation ratio	N/A	0.2540	0.1529	0.7540	[0.05,0.8]
stem_leaf <sup>1</sup>	Stem to leaf allocation ratio	N/A	1.047	1.016	0.754	[0.3,2.2]
leaf_long	Leaf longevity (yr)	0.9744	5 <sup>3</sup>	N/A	N/A	[0.75, 2.0]
slatop	Specific leaf area at canopy top (m <sup>2</sup> gC <sup>-1</sup> )	0.00781	0.00462	0.0128	0.0126	[0.004,0.04]
leafcn	Leaf C to N ratio	35.56	70.17	64.84	33.14	[20,75]
froot_leaf <sup>2</sup>	Fine root to leaf allocation ratio	0.3944	0.8567	0.3211	0.6862	[0.15, 2.0]
mp	Ball-Berry stomatal conductance slope	N/A	7.50	9.32	10.8	[4.5, 12]

422 Optimized values of PFT-specific parameters. The range column values in brackets indicate the range of  
 423 acceptable parameter values used in the sensitivity analysis and the optimization across all four PFTs in the  
 424 format [minimum, maximum]. N/A indicates that parameter is not relevant for that PFT.

425 <sup>1</sup>for tree PFTs, this parameter depends on NPP. The value shown is the allocation at an NPP of 800 gC m<sup>-2</sup>  
 426 yr<sup>-1</sup>.

427 <sup>2</sup> the fine root pool is used as a surrogate for non-photosynthetic tissue in *Sphagnum*

428 <sup>3</sup> This parameter was not optimized; we used the default value.

429

430

431 Table 3: Non PFT-specific optimized model parameters

	Description	Optimized value	Default	Range
r_mort	Vegetation mortality	0.0497	0.02	[0.005, 0.1]
decomp_depth_efolding	Depth-dependence e-folding depth for decomposition (m)	0.3899	0.5	[0.2, 0.7]
q <sub>drai,0</sub>	Maximum subsurface drainage rate (kg m <sup>-2</sup> s <sup>-1</sup> )	3.896e-6	9.2e-6*	[0, 1e-3]
Q <sub>10_mr</sub>	Temperature sensitivity of maintenance respiration	2.212	1.5	[1.2, 3.0]
br_mr	Base rate for maintenance respiration (gC gN m <sup>2</sup> s <sup>-1</sup> )	4.110e-6	2.52e-6	[1e-6, 5e-6]
crit_onset_gdd	Critical growing degree days for leaf onset	99.43	200	[20, 500]
lw_top_ann	Live wood turnover proportion (yr <sup>-1</sup> )	0.3517	0.7	[0.2, 0.85]
gr_perc	Growth respiration fraction	0.1652	0.3	[0.12, 0.4]
r <sub>drai,0</sub>	Coefficient for surface water runoff (kg m <sup>-4</sup> s <sup>-1</sup> )	6.978e-7	8.4e-8*	[1e-9, 1e-6]

432 Optimized and default values for non PFT-specific parameters. The range column values in brackets  
 433 indicate the range of acceptable parameter values used in the sensitivity analysis and the  
 434 optimization in the format [minimum, maximum].

435 \* Previously calibrated value from Shi et al (2015)

436

## 437 4. Results

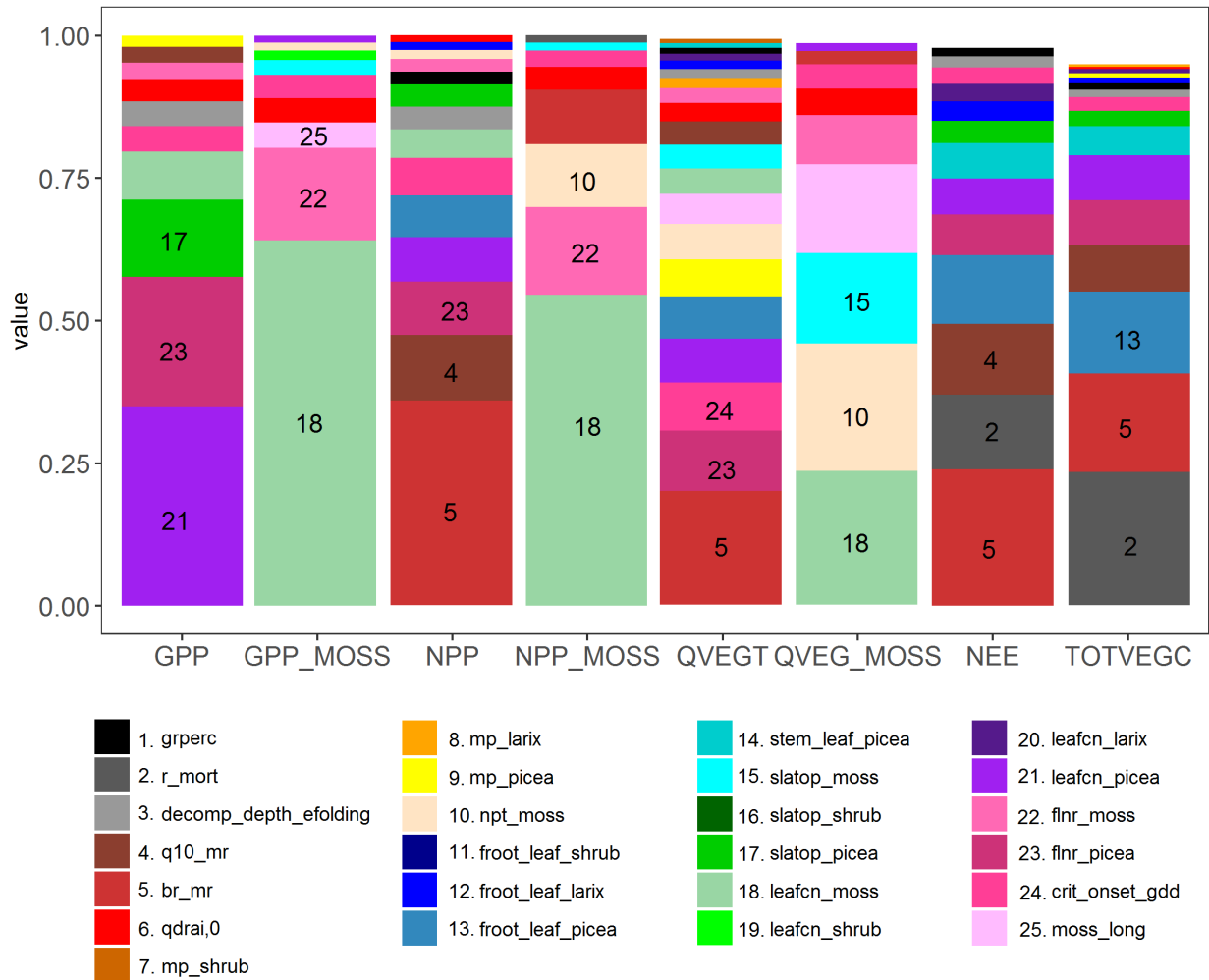
### 438 4.1 Model sensitivity analysis

439 Main effect (first-order) sensitivities are shown for eight model output quantities of  
 440 interest: Total site gross primary productivity (GPP), GPP for the moss PFT only  
 441 (GPP\_moss), total site net primary productivity (NPP), NPP for the moss PFT only  
 442 (NPP\_moss), total site vegetation transpiration (QVEGT), evaporation from the moss  
 443 surface (QVEG\_moss), net ecosystem exchange (NEE) and site total vegetation carbon

444 (TOTVEGC) (Fig. 2). Out of 35 parameters investigated, 25 show a sensitivity index of  
445 at least 0.01 for one of the quantities of interest, and these are plotted on figure 2. In that  
446 figure, sensitivities are stacked in order from highest to lowest for each variable, with the  
447 height of the bar equal to the sensitivity index. The first order sensitivities sum to at least  
448 0.95 for all variables, indicating that higher order sensitivities (i.e., contributions to the  
449 sensitivity from combinations of two or more parameters) contribute relatively little to  
450 the variance for these quantities of interest.

451         According to this analysis, the variance in total site GPP is dominated by three  
452 *Picea* parameters: the fraction of leaf nitrogen in RuBiCO (*flnr\_picea*), leaf carbon to  
453 nitrogen ratio (*leafcn\_picea*) and the specific leaf area at canopy top (*slatop\_picea*). GPP  
454 sensitivity for the moss PFT is dominated by the same three parameters, but for the moss  
455 PFT instead of *Picea* (*flnr\_moss*, *leafcn\_moss*, and *slatop\_moss*). For NPP, QVEGT and  
456 NEE, the highest sensitivity the maintenance respiration base rate *br\_mr*, similar to  
457 earlier results in Griffiths et al. (2017). The maintenance respiration temperature  
458 sensitivity  $Q_{10\_mr}$  is also a key parameter for NPP and NEE. The critical onset growing  
459 degree day threshold (*crit\_onset\_gdd*), which drives deciduous phenology in the spring  
460 for the *Larix* and shrub PFTs, is an important parameter for NPP and NEE. *flnr\_picea* is  
461 important for both NPP and QVEGT. For NPP\_moss and QVEG\_moss, *leafcn\_moss* is  
462 and the ratio of non-photosynthesizing tissue to photosynthesizing tissue (*npt\_moss*) are  
463 sensitive. For TOTVEGC and NEE, vegetation mortality (*r\_mort*) is also a sensitive  
464 parameter. For the site-level quantities of interest, at least 10 parameters contribute  
465 significantly to the uncertainty, illustrating the complexity of the model and large number  
466 of processes contributing to uncertainty in SPRUCE predictions. For the moss variables,

467 there are some cases where significant sensitivities exist for non-moss PFT parameters.  
 468 For example, *leafcn\_shrub* is the seventh most sensitive parameter for GPP\_moss,  
 469 indicating that competition between the PFTs for resources may be important. In this  
 470 case, uncertainty about parameters on one PFT may drive uncertainties in the simulated  
 471 productivity of other PFTs.



472

473 Figure 2 Sensitivity analysis of ELM-SPRUCE for selected parameters (Table 2 and 3). The  
 474 Colored bars indicate the fraction of variance in site gross primary productivity (GPP), moss-only  
 475 NPP (GPP\_MOSS), site net primary productivity (NPP), moss-only NPP (NPP\_MOSS), total  
 476 vegetation transpiration (QVEGT), moss evaporation (QVEG\_MOSS), site net ecosystem  
 477 exchange (NEE) and total vegetation carbon (TOTVEGC) controlled by each parameter. The  
 478 legend shows the top 25 most influential parameters; the remaining parameters not shown have  
 479 sensitivities of no more than 0.01 for any of the outputs. All variables represent 2011-2017

480 average values over the ambient conditions. For parameters that are treated as PFT-dependent,  
481 the PFT is indicated with a suffix (picea, larix, shrub or moss)  
482

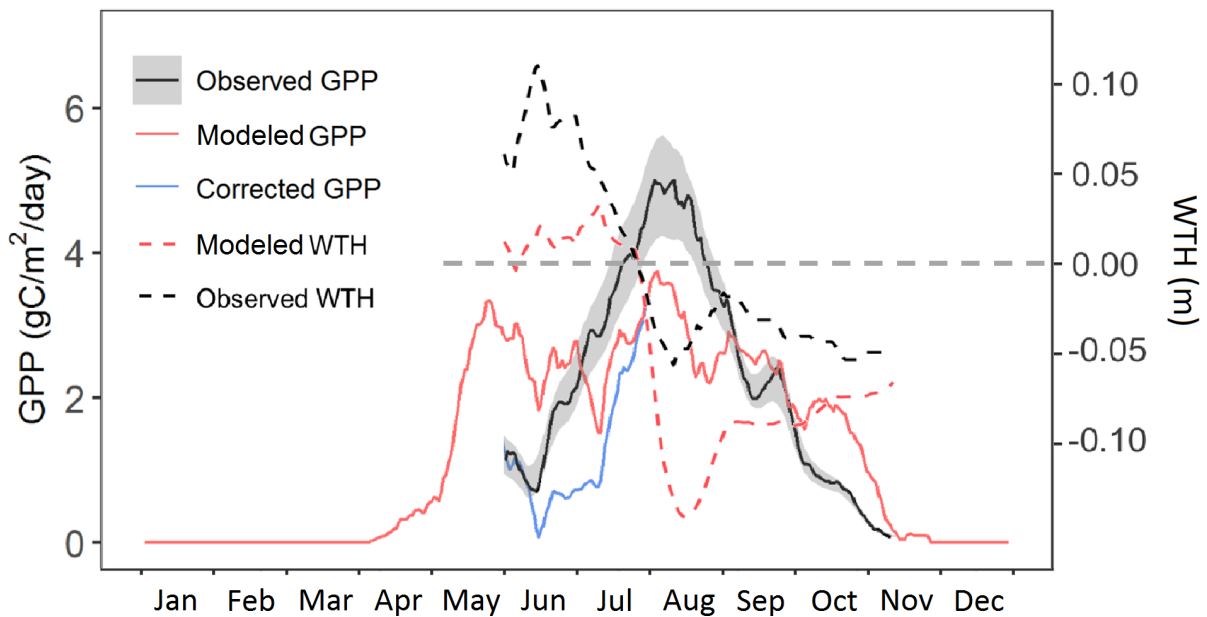
## 483 **4.2 Model evaluation**

484 Our model simulates GPP for vascular plants and *Sphagnum* moss in both  
485 hummock and hollow settings, with separate calculations for each PFT. Here we use the  
486 model estimate of GPP prior to downregulation by nutrient limitation from the ambient  
487 case, based on recent studies indicating that nutrient limitation effects are occurring  
488 downstream of GPP (Raczka et al. 2016; Metcalfe et al., 2017; Duarte et al. 2017). This  
489 treatment of nutrient limitation on GPP has been modified in a more recent version of  
490 ELM, and our moss modifications will be merged to that version as a next step. For now,  
491 by referring to the pre-downregulation GPP we are capturing the most significant impact  
492 of those changes for the purpose of comparison to observations.

493 Our model simulated two seasonal maxima of *Sphagnum* moss GPP, one at the  
494 end of May, and the other in August (Figure 3). Both peaks are lower than the maximum  
495 of observed (flux-partitioned) GPP, which occurs in August. Based on results of the  
496 sensitivity analysis, it could be that the base rate for maintenance respiration for moss is  
497 too high, causing an underestimate of NPP and biomass, which leads to a low bias in  
498 peak GPP.

499 During June and October, observations suggest that ELM\_SPRUCE over-predicts  
500 GPP. The model does limit GPP as a function of the depth of standing water on the bog  
501 surface (Eq. 7). The water table height (WTH) above the bog surface is being predicted  
502 by the model (dashed red line in Fig. 3), and while the seasonal pattern of higher water

503 table in the spring and lower water table in the fall agrees well with observations (dashed  
 504 black line in Fig. 3), the predicted WTH is generally too low by 5-10 cm. The modeled  
 505 WTH here is for hollow. We turned off the lateral transport when there is ice on the soil  
 506 layers above the water table to avoid an unreasonable amount of ice accumulation on the  
 507 frozen layers, which results in there is no flow from hummock to hollow. Forcing the  
 508 modeled GPP to respond to observed WTH (during the period with observations) gives a  
 509 pattern of increasing GPP through June and July which is more consistent with  
 510 observations (blue line in Fig. 3). We do not have observations for GPP earlier than June,  
 511 due to limitations of the instrumentation when the bog surface is flooded.



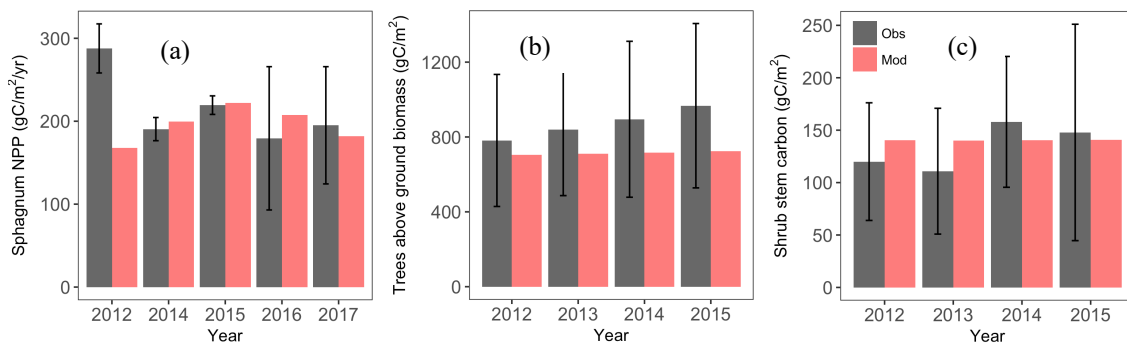
512  
 513  
 514 Figure 3. Predicted GPP (red solid line) compared with flux-partitioned GPP (black solid line,  
 515 GPP data was not used in the parameters optimization) of *Sphagnum* mosses for the year 2014.  
 516 The blue line is the predicted GPP corrected with the observed water table height. The dashed  
 517 black and red lines are observed and modeled water table height (the dashed gray line is the  
 518 hollow surface).

519  
 520  
 521 The model simulated reasonable annual values for *Sphagnum* NPP for the period  
 522 2014-2017 but showed much lower NPP compared with observation (139 vs. 288 g



523 C/m<sup>2</sup>/yr) for the year 2012 (Fig. 4a). Measurement uncertainties are larger in 2016-2017  
 524 than in earlier years, perhaps related to a new measurement protocol for those years, and  
 525 the model estimates are within measurement uncertainty bounds for years 2014-2017  
 526 (Griffiths et al., 2018; Norby et al., 2019). The observed *Sphagnum* NPP was measured at  
 527 different plots and each plot included different species abundances. As a result, the scaled  
 528 NPP includes spatial variations and uncertainty in species distribution (Norby and Childs,  
 529 2017).

530 Simulated tree above ground biomass is within the observed inter-plot variability  
 531 (Fig. 4b). Observations suggest an increasing trend in tree biomass, which was not  
 532 predicted by the model. The optimized parameters show increased mortality and  
 533 autotrophic respiration rate parameters compared to the default model (Table 3), which  
 534 causes the simulations to approach steady state relatively quickly after the 1974  
 535 disturbance. However, the sensitivity analysis also identifies these mortality and  
 536 maintenance respiration parameters as highly sensitive, therefore this simulated response  
 537 is uncertain. For the shrub stem carbon, the simulated mean from year 2012 to 2015 was  
 538 140.4 g C/m<sup>2</sup>, slightly higher than the observation (133.9 g C/m<sup>2</sup>) but well within the  
 539 observed range of inter-plot variability (Fig. 4c).

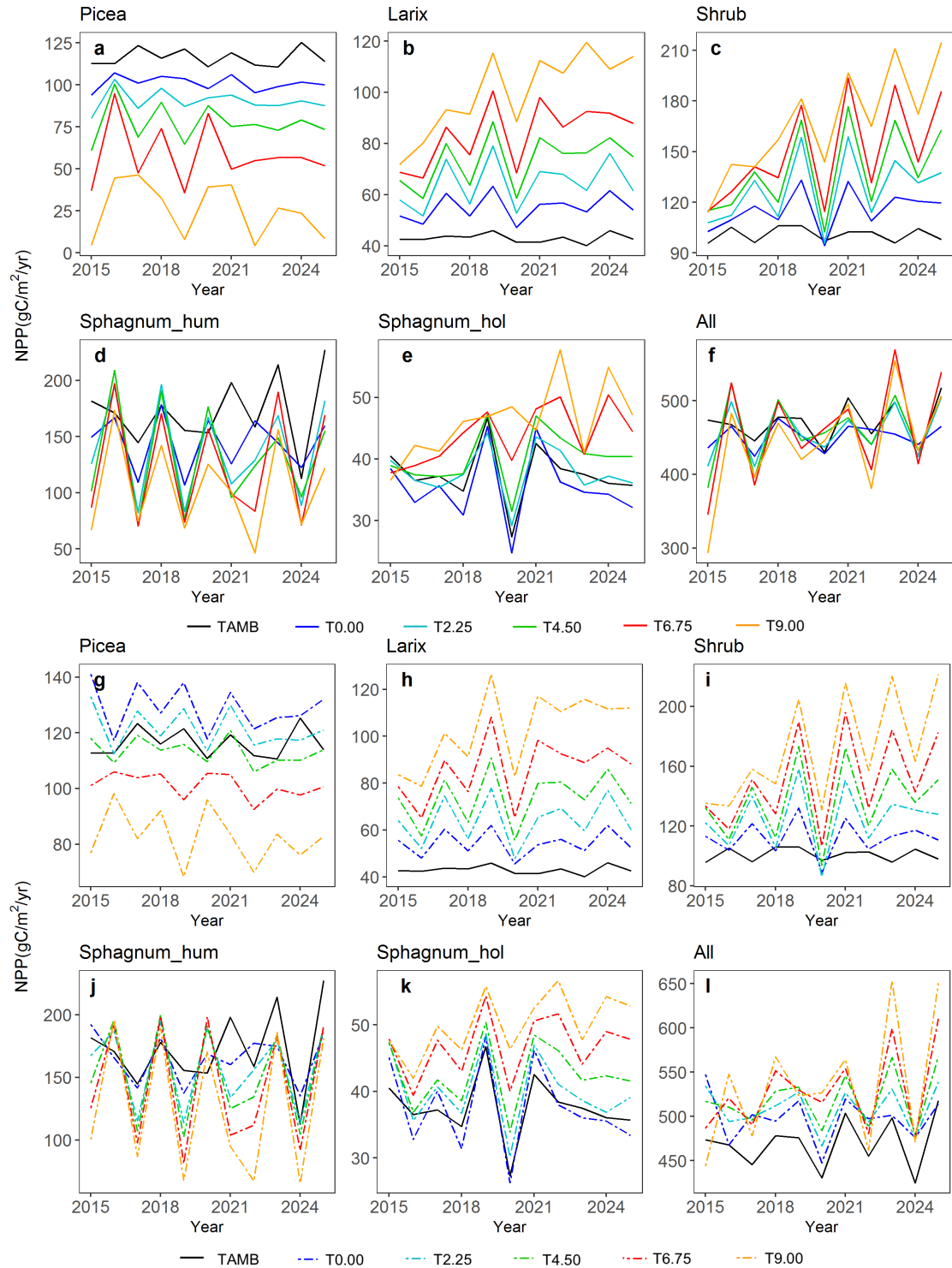


540

541 Figure 4. Predicted (red bars) *Sphagnum* NPP (left), aboveground tree biomass (middle) and  
542 shrub stem carbon (right) compared with the observations (black bars). Observed NPP data are  
543 based on growth of 12-17 bundles of 10 *Sphagnum* stems in 2012-2015 (unpublished data) and  
544 in two ambient plots by the method described by Norby et al. (2019) in 2016-2017 (data in  
545 Norby et al. 2017). The *Sphagnum* NPP data of year 2015-2017, and aboveground tree biomass  
546 and shrub stem carbon of year 2014-2015 are independent of the related parameters  
547 optimization.

### 549 **4.3 Simulated carbon cycle response to warming and elevated atmospheric CO<sub>2</sub>** 550 **concentration**

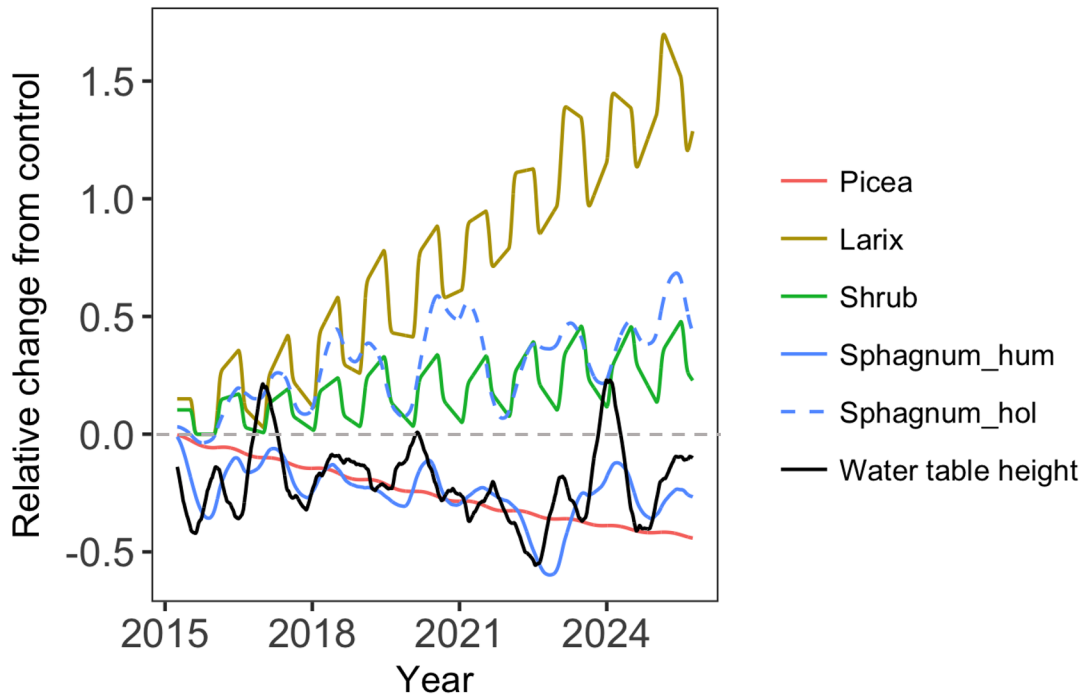
551 Different PFTs demonstrated different warming responses for both ambient CO<sub>2</sub>  
552 and elevated CO<sub>2</sub> concentration conditions (Fig. 5). Both *Larix* and shrub NPP increased  
553 with warming under both CO<sub>2</sub> concentration conditions (Fig. 5 b, c, h and i). In addition,  
554 CO<sub>2</sub> fertilization stimulates the growth of these two PFTs and the fertilization effect  
555 further increases with warming (Fig. S1). In contrast, *Picea* NPP decreased with warming  
556 levels (Fig. 5 a and g) for both CO<sub>2</sub> conditions. For *Sphagnum*, NPP decreased in  
557 hummocks but increased in hollows with increasing temperature (Fig. 5 d, e, j and k).  
558 The CO<sub>2</sub> fertilization also stimulates the growth of the *Picea* and *Sphagnum* PFTs (Fig. 5 a,  
559 d, e, g, j and k). The enclosure-total NPP for all PFTs responded differently to the  
560 warming only and warming with elevated CO<sub>2</sub> (Fig. 5 f and l). The enclosure-total NPP  
561 for each warming level changed less under the ambient CO<sub>2</sub> condition than those with  
562 elevated CO<sub>2</sub> condition, and NPP decreased with warming in most of years under  
563 ambient CO<sub>2</sub> condition but increased under elevated CO<sub>2</sub> condition (Fig. 5 f and l). This  
564 result demonstrated that the elevated CO<sub>2</sub> scenario changes the sign of the NPP warming  
565 response for the bog peatland ecosystem.



566  
 567  
 568  
 569  
 570  
 571

Figure 5 predicted NPP response to warming with ambient atmospheric CO<sub>2</sub> (a-f, solid lines) and warming with elevated atmospheric CO<sub>2</sub> concentration (g-l, dash lines), the black solid line TAMB is the ambient temperature and CO<sub>2</sub> case, T0.00 to T9.00 means increasing temperature from 0°C to 9°C

572 Compared with the ambient biomass, the biomass of black spruce (*Picea*)  
573 significantly decreased but the biomass of *Larix* significantly increased under the greatest  
574 warming treatment (+9.00°C, Fig.6). Biomass of shrub and hollow *Sphagnum* also  
575 increased, but less than did *Larix*. The hummock *Sphagnum* biomass also showed strong  
576 correlation with water table height at roughly a 3-month lag (the maximum correlation  
577 occurs with an 82-day lag,  $R^2=0.56$ ). NPP is allocated instantaneously into biomass. A  
578 positive NPP anomaly caused by water table shifts leads to higher LAI, which also  
579 increases future productivity for some amount of time even if the water table returns to  
580 normal. *Sphagnum* biomass has a 1-year turnover time in the simulation. This  
581 combination of effects leads to a roughly 3-month timelag. Due to the relative lower  
582 height of the water table in the hummock than the hollow, the simulated hummock  
583 *Sphagnum* were more significantly water-stressed than the hollow *Sphagnum* as the water  
584 table height declines. This is consistent with multiple studies finding an increase in  
585 temperatures associated with drought (low water table height) reducing *Sphagnum*  
586 growth (Bragazza et al., 2016; Granath et al., 2016; Mazziotta et al., 2018). We plotted  
587 the predicted canopy evaporation for hummock and hollow *Sphagnum* responses to  
588 warming and found that both hummock and hollow *Sphagnum* canopy evaporation  
589 increase with warming for both ambient and elevated atmospheric CO<sub>2</sub> conditions despite  
590 the *Larix* and shrubs are growing with warming. Moreover, the hollow *Sphagnum* canopy  
591 evaporation warming response is stronger than that of the hummock *Sphagnum* (Fig. S2).  
592 In summary, the growth of bog vegetation is predicted to have species-specific warming  
593 responses that differ in sign and magnitude.



594  
 595 Figure 6 The relative changes of biomass for different PFTs and water table height (the weighted  
 596 average between hummock and hollow) between +9.00 °C treatment case and the ambient case  
 597 (+9.00 °C / ambient - 1)

598 **5. Discussion**

599  
 600 *Sphagnum* moss is the principal plant involved in the peat accumulation in peatland  
 601 ecosystems, and effective characterization of its biophysical and physiological responses  
 602 has implications for predicting peatland and global carbon, water and climate feedbacks.  
 603 This study moves us closer to our long-term goal of improving the prediction of peatland  
 604 water, carbon and nutrient cycles in ELM\_SPRUCE, by introducing a new *Sphagnum*  
 605 moss PFT, implementing water content dynamics and photosynthetic processes for this  
 606 nonvascular plant. The *Sphagnum* model development combined with our previous  
 607 hummock-hollow microtopography representation and laterally-coupled two-column  
 608 hydrology scheme enhance the capability of ELM\_SPRUCE in simulating high-carbon  
 609 wetland hydrology and carbon interactions and their responses to plausible environmental  
 610 changes.

611

## 612 **5.1 Uncertainties in simulating *Sphagnum* productivity**

613           Our predicted peak GPP is similar to the results found by Walker et al. (2017)  
614 when they calculated the internal resistance to CO<sub>2</sub> diffusion as a function of *Sphagnum*  
615 water content using a stand-alone photosynthesis model. In both cases, the predicted peak  
616 GPP is lower than observations. Walker et al. (2017) were, however, able to capture the  
617 observed peak magnitude with a combination of light extinction coefficient, canopy  
618 clumping coefficient, maximum SAI, and a logistic function describing the effective  
619 *Sphagnum* SAI in relation to water table. Here we used model default values for the light  
620 extinction and canopy clumping coefficients. While the water table impacts *Sphagnum*  
621 productivity in our simulation, modeled LAI is mainly controlled by NPP and turnover.  
622 In addition, we use the default formulation for acclimation of V<sub>cmax</sub> in ELM which is  
623 based on a 10-day mean growing temperature. At this point we don't have sufficient  
624 measurements to test this assumption, but we can prioritize these measurements in the  
625 future. *Sphagnum* temperature is computed from surface energy balance but because the  
626 current model doesn't estimate the shading effects from trees and shrubs, this may be  
627 overestimated. Moreover, biases in predicted water table height contribute to errors in  
628 the calculated submergence effect. Improving these biases and assuming an exponential  
629 rather than a linear CO<sub>2</sub> uptake profile may improve representation of the submergence  
630 effect. All these aspects may be attribute to the biases of the simulated *Sphagnum* GPP.  
631 We can consider this in the future when we have more detailed measurements. Further  
632 investigation is thus needed to understand how representative the chamber-based  
633 observations from Walker et al. (2017) are of the larger-scale SPRUCE enclosures, and to  
634 reconcile these GPP estimates with plot-level NPP observations (Norby et al., 2019).

635           The hydrology cycle, especially water table depth (WTD) is also a key factor that  
636 influences the seasonality of GPP in *Sphagnum* mosses (Lafleur et al., 2005; Riutta 2007,  
637 Sonnentag et al, 2010; Grant et al., 2012; Kuiper et al., 2014; Walker et al, 2017). One  
638 key feedback is if the water table declines, there can be enhanced decomposition and  
639 subsidence of the peat layer, which brings the surface down closer to the water table  
640 again. But we currently did not consider the peat layer elevation changes in our model  
641 and this will be one of the future development directions. The capillary rise plays into the  
642 *Sphagnum* hydrological balance, which varies depending on water table depth and  
643 evaporative demand. At short timescales or under rapidly changing conditions, there may  
644 not be equilibration between the *Sphagnum* water content and the peat moisture.  
645 Generally, the *Sphagnum* water content will equilibrate with the peat on a daily basis  
646 outside the plot since the dew point is often reached at night. But since the vapor pressure  
647 deficit does not go to zero inside the warmer plots, some disequilibrium could remain.  
648 High-frequency latent heat flux data from the site are currently lacking, but could help to  
649 constrain these effects in the future.

650           The current phenology observations also include if *Sphagnum* hummock and hollow  
651 are wet or dry, and we could look at the relationship with soil water content sensors in the  
652 future. Moreover, the timescales for rewetting may change as the peat dries since the  
653 cross section for capillary rise will decline and thus the maximum flux to the surface will  
654 decline. At some point, between gravity potential and reduced hydraulic conductivity, we  
655 expect that the capillarity will no longer satisfy evaporative demand. Alternately, under  
656 saturated conditions when the water table is close to the *Sphagnum* surface, *Sphagnum*  
657 photosynthesizing tissue can become submerged or surrounded by a film of water that is

658 likely to reduce the effective LAI of the *Sphagnum* and thus reduce photosynthesis  
659 (Walker et al., 2017). Submerged *Sphagnum* can take up carbon derived from CH<sub>4</sub> via  
660 symbiotic methanotrophs (Raghoebarsing et al., 2005), but in any cases CO<sub>2</sub> diffusion for  
661 photosynthesis will dramatically decrease under water. Larmola et al. (2014) also  
662 reported that the activity of oxidizing bacteria provides not only carbon but also nitrogen  
663 to peat mosses and, thus, contributes to carbon and nitrogen accumulation in peatlands,  
664 which store approximately one-third of the global soil carbon pool. We currently didn't  
665 consider this kind of CH<sub>4</sub> associated carbon and nitrogen uptake by *Sphagnum*.

666         The live green *Sphagnum* moss layer buffers the exchange of energy and water at  
667 soil surface and regulates the soil temperature and moisture because of its high-water  
668 holding capacity and the insulating effect (McFadden et al., 2003; Block et al., 2011;  
669 Turesky et al, 2012; Park et al., 2018). Currently, we apply the same method for the  
670 hummock and hollow *Sphagnum* water content prediction and can test the model against  
671 the measured data when more data are available. Our model still can predict *Sphagnum*  
672 water content differences between these microtopographies as expected, with the water  
673 content of hollows greater than that of hummocks though. In addition, our model is able  
674 to represent the self-cooling effect, although we do not yet have measurements available  
675 to validate the model. The relationship of the differences between vegetation temperature  
676 (TV) and 2m air temperature (TBOT) (TV-TBOT) and canopy evaporation for both  
677 hummock and hollow *Sphagnum* demonstrated that the differences of TV-TBOT was  
678 negative and the canopy evaporation had a negative relationship with TV-TBOT (Fig.  
679 S3). Moreover, Walker et al., (2017) reported that the function of *Sphagnum* water  
680 content to soil water content or to water table depth they used for the SPRUCE site was



681 empirical and may not be representative for peatland ecosystem. To better represent the  
682 peatland ecosystem in our model, we will eventually treat the *Sphagnum* mosses as the  
683 “top” soil layer with a lower thermal conductivity and higher hydraulic capacity  
684 (Beringer et al., 2001; Wu et al., 2016; Porada et al., 2016).

685

## 686 **5.2 Predicted warming and elevated CO<sub>2</sub> concentration response uncertainties**

687

688 Our model warming simulations suggested that increasing temperature reduced  
689 the *Picea* growth but increased the growth of *Larix* under both ambient and elevated  
690 atmospheric CO<sub>2</sub> conditions. The main reason for this model difference in response for  
691 the two tree species is that despite their similar productivity under ambient conditions,  
692 *Picea* has more respiring leaf and fine root biomass because of lower SLA, longer leaf  
693 longevity, and higher fine root allocation. Therefore, warming results in a much larger  
694 increase in maintenance respiration relative to changes in NPP for *Picea* compared to  
695 *Larix* (Fig. 5 and Fig. S4). Increased tree growth and productivity in response to the  
696 recent climate warming for high-latitude forests has been reported (Myneni et al., 1997,  
697 Chen et al. 1999, Wilming et al. 2004, Chavardes, 2013). On the other hand, reductions in  
698 tree growth and negative correlations between growth and temperature also have been  
699 shown (Barber et al., 2000; Wilmking et al., 2004; Silva et al., 2010; Juday and Alix  
700 2012; Girardin et al., 2016; Wolken et at., 2016).

701 Our model also predicted increasing growth of shrubs with increased temperature,  
702 similar to simulated increase in shrub cover caused mainly by warmer temperatures and  
703 longer growing seasons reported by Miller and Smith (2012) using their model LPJ-  
704 GUESS. In addition, several other modelling studies have also found increased biomass

705 production and LAI related to shrub invasion and replacement of low shrubs by taller  
706 shrubs and trees in response to increased temperatures in tundra regions (Zhang et al.,  
707 2013; Miller and Smith, 2012; Wolf et al., 2008; Porada et al., 2016; Rydssa et al., 2017).

708 The responses of *Sphagnum* mosses to warming simulated by ELM\_SPRUCE  
709 showed that *Sphagnum* growth in hollows was consistently higher with increased  
710 temperatures, where water availability was not limiting. *Sphagnum* growing on  
711 hummocks, on the other hand, showed negative warming responses that are related to the  
712 strong dependency on water table height. A Recent study of the same SPRUCE site  
713 (Norby et al. 2019) had suggested that the hummock-hollow microtopography had a  
714 larger influence on *Sphagnum* responses to warming than species-specific traits. In  
715 addition, the previous studies had demonstrated that the most dominant mechanism of  
716 *Sphagnum* warming response was probably through the effect of warming on depth to the  
717 water table and water content of the acrotelm, both of them responded to increasing  
718 temperature (Grosvernier et al., 1997; Rydin, 1985; Weltzin et al., 2001; Norby et al.,  
719 2019). Moreover, desiccation of capitula due to increased evaporation associated with  
720 higher temperatures and vapor pressure deficits can reduce *Sphagnum* growth  
721 independent of the water table depth (Gunnarsson et al., 2004). We currently used the  
722 same parameters for both hummock and hollow, but could consider species differences in  
723 the future. Norby et al. (2019) investigated different *Sphagnum* species at the same site  
724 and reported there was no support for the hypothesis that species more adapted to dry  
725 conditions (e.g., *S. magellanicum* and *Polytrichum* mainly on hummocks) would be more  
726 resistant to the stress and would increase in dominance, and both hummock and hollow  
727 *Sphagnum* are declining with warming despite the differences between them. This

728 declining trend may be in part due to increased shading from the shrub layer, which is  
729 expanding with warming (McPartland et al., 2020).

730 Ecosystem warming can have direct and indirect effects on *Sphagnum* moss  
731 growth. The growth of *Sphagnum* may be reduced directly by higher air temperature, due  
732 to the relatively low temperature optima of moss photosynthesis (Hobbie et al., 1999; Van  
733 Gaalen, 2007; Walker et al., 2017). On the other hand, increased shading by the shrub  
734 canopy and associated leaf litter could indirectly decrease moss growth (Chapin et al.,  
735 1995; Hobbie and Chapin 1998; Van der Wal et al., 2005; Walker et al., 2006; Breeuwer  
736 et al., 2008). In contrast, other studies suggest that *Sphagnum* growth can be promoted  
737 via a cooling effect of shading on the peat surface, by alleviating photo-inhibition of  
738 photosynthesis and also by reducing evaporation stress (Busby et al., 1978; Murray et al.,  
739 1993; Man et al., 2008; Walker et al., 2015, Bragazza et al., 2016, Mazziotta et al., 2018).  
740 Our model sensitivity analysis also indicated that the parameters of Shrub showing  
741 significant sensitivities to *Sphagnum* mosses GPP, indicating that competition between  
742 the PFTs for resources might be important. Moreover, ELM\_SPRUCE did predict  
743 enhancement of shrub and *Larix* tree with increased temperatures with both ambient and  
744 elevated CO<sub>2</sub> conditions (LAI increasing with warming, Fig. S5). Currently  
745 ELM\_SPRUCE does not include light competition among multiple PFTs, and thus does  
746 not represent cross-PFT shading effects, which may contribute to the warming and  
747 elevated CO<sub>2</sub> response differences between our model prediction and observed result of  
748 Norby et al. (2019). Meanwhile, we have fixed cover fraction for PFTs in our model may  
749 also contribute to the disagreement of predicted and observed warming responses. While

750 Norby et al. (2019) showed that the fractional cover of different *Sphagnum* species  
751 declined with warming.

752 *Sphagnum* mosses are sitting on top of high CO<sub>2</sub> sources. CH<sub>4</sub> can be a significant  
753 carbon sources of submerged *Sphagnum* (Raghoebarsing et al., 2005; Larmola et al,  
754 2014); refixation of CO<sub>2</sub> derived from decomposition processes also is an important  
755 source of carbon for *Sphagnum* (Rydin and Clymo, 1989; Turetsky and Wieder, 1999).

756 The effects of the elevation of atmospheric CO<sub>2</sub> on *Sphagnum* moss are currently  
757 disputed, with studies indicating an increase in growth rate (Jauhiainen and Silvde 1999;  
758 Heijmans et al. 2001a; Saarnio et al. 2003), decreases in growth rate (Grosvernier et al.  
759 2001; Fenner et al. 2007) and no response (Van der Hejiden et al. 2000; Hoosbeek et al.  
760 2002; Toet et al. 2006). Norby et al. (2019) indicated that no growth stimulation of both  
761 hummock and hollow *Sphagnum* under elevated CO<sub>2</sub> condition, but significant negative  
762 effects of elevated CO<sub>2</sub> on *Sphagnum* NPP in year 2018 at the same study site.

763 Contrasting responses between *Sphagnum* species are thought to be coupled with the  
764 water availability. In contrast, our model results showed that both hummock and hollow  
765 *Sphagnum* growths were stimulated by the elevated CO<sub>2</sub> concentration, which may be  
766 attributed to the fact that we did not consider the light competition between the PFTS  
767 (shrub and tree shading effects) and use a fixed cover fraction of *Sphagnum*.

768 The CO<sub>2</sub> vertical concentration profile is assumed to be uniform in the  
769 simulations. In the experiment, the enclosure's regulated additions of pure CO<sub>2</sub> are  
770 distributed to a manifold that splits the gas into four equal streams feeding each of the  
771 four air handling units (Hanson et al., 2017 Fig. 2a), and is injected into the ductwork of  
772 each furnace just ahead of each blower and heat exchanger. Horizontal and vertical

773 mixing within each enclosure homogenizes the air volume distributing the CO<sub>2</sub> along  
774 with the heated air. The horizontal blowers in the enclosures together with external wind  
775 eddies ensure vertical mixing. We do not have routine automated CO<sub>2</sub> concentration data  
776 below 0.5m. The moss layer may well be experiencing higher concentrations than  
777 assumed by the model, but such an impact will be minimized during daylight hours.  
778 Preliminary isotopic measurements imply a significant fraction of carbon assimilated by  
779 the moss may come from subsurface respired CO<sub>2</sub> (i.e., CO<sub>2</sub> with older 14C signatures  
780 predating bomb carbon that can only be sourced from deeper peat, Hanson et al., 2017).  
781 However, the observed elevated CO<sub>2</sub> response is smaller than simulated (Hanson et al.,  
782 2020). [Understanding the drivers of elevated CO<sub>2</sub> response or lack thereof is a key topic](#)  
783 [for future work.](#)

784 To better investigate the *Sphagnum* warming and elevated CO<sub>2</sub> responses, we should  
785 also focus on revealing the interactions with shrub and nitrogen availability (Norby et al.,  
786 2019). Nitrogen (N<sub>2</sub>) fixation is a major source of available N in ecosystems that receive  
787 low amounts of atmospheric N deposition, like boreal forests and subarctic tundra (Lindo  
788 et al., 2013, Weston et al, 2015, Rousk et al., 2016, Kostka et al., 2016). For example,  
789 diazotrophs are estimated to supply 40-60% of N input to peatlands (Vile et al., 2014)  
790 with high accumulation of fixed N into plant biomass (Berg et al., 2013). Nevertheless,  
791 N<sub>2</sub> fixation is an energy costly process and is inhibited when N availability and reactive  
792 nitrogen deposition is high (Gundale et al., 2011; Ackermann et al., 2012; Rousk et al.,  
793 2013). This could limit ecosystem N input via the N<sub>2</sub> fixation pathway. We are measuring  
794 *Sphagnum* associated N<sub>2</sub> fixation at the SPRUCE site and found that rates decline with  
795 increasing temperature (Carrell et al. 2019 Global Change Biology). We are continuing

796 these measurements to see if they correlate with the GPP empirical relationship from  
797 Cleveland et al. (1999), or if temperature disrupts that association. Once finished, results  
798 will be used to represent N fixation by the *Sphagnum* layer and testing with  
799 measurements.

800         It is also encouraging that while we did not use leaf-level gas exchange  
801 observations in our optimization, the increased maintenance respiration base rate and  
802 temperature sensitivity compared to default (table 2) is largely consistent with pre-  
803 treatment leaf level observations (Jensen et al., 2019). In the future, a multi-scale  
804 optimization framework that can assimilate leaf and plot-level observations  
805 simultaneously should lead to improved model predictions and reduced uncertainties for  
806 the treatment simulations. If similar patterns observed in ambient conditions continue  
807 during the treatments, incorporating seasonal variations in leaf photosynthetic parameters  
808 may also further improve the simulated response to warming (Jensen et al., 2019).

809         Overall, while the sensitivity analysis is useful to indicate the key parameters and  
810 mechanisms responsible for uncertainty, our ability to quantify prediction uncertainty is  
811 limited because we consider only a single simulation with optimized parameters. Ideally,  
812 we should perform a model ensemble that represents the full range of posterior  
813 uncertainty over simulations that are consistent with the pre-treatment observations, and  
814 also a range of possible future meteorological conditions. This is currently being done for  
815 SPRUCE with the TECO carbon cycle model (Jiang et al., 2018), but the computational  
816 expense of ELM\_SPRUCE currently prohibits this approach. By combining new  
817 surrogate modeling approaches (e.g. Lu et al., 2019) with MCMC techniques, it may be  
818 possible to achieve this in the near future. This will help to reduce prediction

819 uncertainties, which currently prevail in the future carbon budget of peatlands and its  
820 feedback to climate change (McGuire et al., 2009).

821         The algorithms used to represent moss (Williams and Flanagan, 1998) are  
822 transferable to and have been applied by other modeling groups in other  
823 peatlands. However, we expect that certain parameters will vary, for example, the  
824 microtopographic parameters, the relationship between peat moisture and internal water  
825 content, and moss properties such as C:N ratio. The parameter sensitivity analysis  
826 informs us as to the most important parameters responsible for prediction uncertainty,  
827 and can inform how to prioritize these measurements. Collecting these measurements  
828 from a variety of sites will be a necessary preliminary exercise. In addition to the  
829 simulations aimed at improved understanding of bog response to experimental  
830 manipulations at the plot-scale, we are pursuing model implementations at larger spatial  
831 scales. The model framework described in this study is capable of performing regional  
832 simulations, although the current simulations were designed for mechanistic  
833 understanding of *Sphagnum* mosses hydrological and physiological dynamics at the plot-  
834 level.

835

## 836 **6. Summary**

837         In this study, we reported the development of a *Sphagnum* moss PFT and  
838 associated processes within the ELM\_SPRUCE model. Before being used to examine the  
839 ecosystem response to warming and elevated CO<sub>2</sub> at a temperate bog ecosystem, the  
840 updated model was evaluated against the observed *Sphagnum* GPP and annual NPP,  
841 aboveground tree biomass and shrub stem biomass. The new model can capture the

842 seasonal dynamics of moss *Sphagnum* GPP, but with lower peak GPP compared to site-  
843 level observations, and can predict reasonable annual values for *Sphagnum* NPP but with  
844 lower interannual variation. Our model largely agrees with observed tree and shrub  
845 biomass. The model predicts that different PFTs responded differently to warming levels  
846 under both ambient and elevated CO<sub>2</sub> concentration conditions. The NPP of the two  
847 dominant tree PFTs (black spruce and *Larix*) showed contrasting responses to warming  
848 scenarios (increasing with warming for *Larix* but decreasing for black spruce), while  
849 shrub NPP had similar warming response to *Larix*. Hummock and hollow *Sphagnum*  
850 showed opposite warming responses: hollow *Sphagnum* shows generally higher growth  
851 with warming, but the hummock *Sphagnum* demonstrates more variability and strong  
852 dependence with water table height. The ELM predictions further suggest that the effects  
853 of CO<sub>2</sub> fertilization can change the direction of the warming response for the bog  
854 peatland ecosystem, though observations of *Sphagnum* species at the site does not yet  
855 appear to support this (Norby et al. 2019).

856 Data availability. The model code we used is available here:  
857 [https://github.com/dmricciuto/CLM\\_SPRUCE](https://github.com/dmricciuto/CLM_SPRUCE). The datasets and scripts were used for the figures  
858 is here: [https://github.com/dmricciuto/CLM\\_SPRUCE/tree/master/analysis/Shietal2020](https://github.com/dmricciuto/CLM_SPRUCE/tree/master/analysis/Shietal2020)  
859  
860

## 861 **Acknowledgements**

862 Research was supported by the U. S. Department of Energy, Office of Science,  
863 Biological and Environmental Research Program. Oak Ridge National Laboratory is  
864 managed by UT-Battelle, LLC, for the US Department of Energy under contract DE-  
865 AC05-00OR22725.

866



867 **References:**

- 868 Ackermann, K., Zackrisson, O., Rousk, J., Jones, D. L., and DeLuca, T. H.: N<sub>2</sub> fixation  
869 in feather mosses is a sensitive indicator of N deposition in boreal forests, *Ecosystems*,  
870 15, 986-998, 2012.
- 871 Barber, V. A., Juday, G. P., and Finney, B. P.: Reduced growth of Alaskan white spruce  
872 in the twentieth century from temperature-induced drought stress, *Nature*, 405,668-  
873 673, 2000.
- 874 Beringer, J., Lynch, A., Chapin, F., Mack, M., and Bonan, G.: The Representation of  
875 Arctic Soils in the Land Surface Model: The Importance of Mosses, *J. Climate*, 14,  
876 3324-3335, doi:10.1175/1520-0442(2001)014<3324:TROASI>2.0.CO;2, 2001.
- 877 Berg, A., Danielsson, A., and Sevansson, B.H.: Transfer of fixed-N from N<sub>2</sub>-fixing  
878 cyanobacteria associated with moss sphagnum riparium results in enhanced growth of  
879 the moss, plant and soil, 362, 271-278, <https://doi.org/10.1007/s11104-012-1278-4>,  
880 2013.
- 881 Blok, D., Heijmans, M., Schaepman-Strub, G., Van Ruijven, J., Parmentier, F.,  
882 Maximov, T., and Berendse, F.: The cooling capacity of mosses: Controls on water  
883 and energy fluxes in a Siberian tundra site, *Ecosystems*, 14, 1055-1065, 2011.
- 884 Bond-Lamberty, B., Peckham, S. D., Ahl, D. E., and Gower, S. T.: Fire as the dominant  
885 driver of central Canadian boreal forest carbon balance, *Nature*, 450, 89-92, 2007.
- 886 Bragazza, L., Buttler, A., Robroek, B. J., Albrecht, R., Zaccone, C., Jassey, V. E., and  
887 Signarbieux, C.: Persistent high temperature and low precipitation reduce peat carbon  
888 accumulation, *Global Change Biology*, 22, 4114-4123,  
889 <https://doi.org/10.1111/gcb.13319>, 2016.
- 890 Breeuwer, A., Heijmans, M. M., Robroek, B. J., and Berendse, F.: The effect of  
891 temperature on growth and competition between Sphagnum  
892 species, *Oecologia*, 156(1), 155-167, doi:10.1007/s00442-008-0963-8, 2008.
- 893 Brown, S. M., Petrone, R. M., Mendoza, C., and Devito, K. J.: Surface vegetation  
894 controls on evapotranspiration from a sub-humid Western Boreal Plain wetland,  
895 *Hydrological Processes*, 24(8), 1072-1085, 2010.
- 896 Busby, J.R., Bliss, L.C., and Hamilton, C.D.: Microclimate control of growth rates and  
897 habitats of the Boreal Forest Mosses, *Tomenthypnum nitens* and *Hylocomium*  
898 *splenden*, *Ecol Monogr*, 48, 95-110, 1978.
- 899 Burrows, S.M., Maltrud, M.E., Yang, X., Zhu, Q., Jeffery, N., Shi., X., Ricciuto, D.M.,  
900 Wang, S., Bisht, G., Tang, J., Wolfe, J. D., Harrop, B. E., Singh, B., Brent, L., Zhou,  
901 Tian, Cameron-Smith P. J., Keen, N., Collier, N., Xu, M., Hunke, E.C., Elliott, S.M.,  
902 Turner, A.K., Li, H., Wang, H., Golaz, J.-C., Bond-Lamberty, B., Hoffman, F.M.,  
903 Riley, W.J., Thornton, P.E., Calvin, K., and Leung, L.R.: The DOE E3SM coupled

- 904 model v1.1 biogeochemistry configuration: overview and evaluation of coupled  
 905 carbon-climate experiments, *J. Adv. Model Earth Sy.*, 12, e2019MS001766,  
 906 <https://doi.org/10.1029/2019MS001766>, 2020.
- 907 Gorham, E.: Northern peatlands: role in the carbon cycle and probable responses to  
 908 climatic warming, *Ecological Applications*, 1, 182-195, 1991.
- 909 Camill, P. and Clark, J. S.: Long-term perspectives on lagged ecosystem responses to  
 910 climate change: permafrost in boreal peatlands and the grassland/woodland boundary,  
 911 *Ecosystems*, 3, 534–544, 2000.
- 912 Chadburn, S., Burke, E., Essery, R., Boike, J., Langer, M., Heiken- feld, M., Cox, P., and  
 913 Friedlingstein, P.: An improved representa- tion of physical permafrost dynamics in  
 914 the JULES land-surface model, *Geosci. Model Dev.*, 8, 1493–1508, doi:10.5194/gmd-  
 915 8- 1493-2015, 2015.
- 916 Chapin, F. S. III, Shaver, G.R., Giblin, A.E., Nadelhoffer, K.J., and Laundre, J.A.:  
 917 Responses of Arctic tundra to experimental and observed changes in climate, *Ecology*,  
 918 76, 694-711, 1995.
- 919 Carrell, A.A., Kolton, M., Warren, M.J., Kostka, J.E., and Weston, D. J.: Experimental  
 920 warming alters the community composition, diversity, and N<sub>2</sub> fixation activity of peat  
 921 moss (*Sphagnum fallax*) microbiomes, *Glob. Change Biol.*, 25, 2993-3004,  
 922 doi:10.1111/gcb.14715, 2019.
- 923 Chavardes, R. D., Daniels, L. D., Waeber P. O., Innes, J. L., and Nitschke, C. R.:  
 924 Unstable climate-growth relations for white spruce in southwest Yukon, Canada,  
 925 *Climatic Change*, 116, 593-611, 2013.
- 926 Chen, W. J., Black, T. A., Yang, P.C. Barr, A.G. Neumann, H. H., Nešić, Z., Blanken, P.  
 927 D. Novak, M. D., Eley, J., Ketler, R., and Cuenca, R. H.: Effects of climatic variability  
 928 on the annual carbon sequestration by a boreal aspen forest, *Glob. Change Biol.*, 5, 41-  
 929 53, 1999.
- 930 Cleveland, C. C., Townsend, A. R., Schimel, D., S., Fisher, H., Howarth, Lars O., H.,  
 931 Perakis, S. S., Latty, E. F., Von Fishcher, J. C., Elseroad, A., and Wasson, M. F.:  
 932 Global patterns of terrestrial biological nitrogen (N<sub>2</sub>) fixation in natural ecosystem,  
 933 *Global Biogeochemical Cycles*, 13(2), 623-645, 1999.
- 934 Clymo, R. S. and Hayward, P.M.: The ecology of *Sphagnum*, in: *Bryophyte Ecology*,  
 935 edited by: Smith, A. I. E., Chapman and Hall Ltd., London, New York, 229-289, 1982.
- 936 Collatz, G.J., Ball, J.T., Grivet, C. and Berry, J.A.: Physiological and environmental-  
 937 regulation of stomatal conductance, photosynthesis and transpiration - a model that  
 938 includes a laminar boundary-layer, *Agricultural and Forest Meteorology*, 54, 107-  
 939 136, 1991.
- 940 Collatz, G.J., Ribas-Carbo, M. and Berry, J.A.: Coupled photosynthesis- stomatal model  
 941 for leaves of C<sub>4</sub> plants, *Australian Journal of Plant Physiology*, 19, 519-538, 1992.

- 942 Cornelissen, H.C., Lang, S.I., Soudzilovskaia, N.A., and During, H.J.: Comparative  
943 cryptogam ecology: a review of bryophyte and lichen traits that drive  
944 biogeochemistry, *Annals of Botany*, 99, 987–1001, 2007.
- 945 Davidson, E. A. and Janssens, I. A.: Temperature sensitivity of soil carbon decomposition  
946 and feedbacks to climate change, *Nature*, 440, 165-173, 2006.
- 947 Dorrepaal, E., Toet, S., van Logtestijn, R. S. P., Swart, E., van de Weg, M. J., Callaghan,  
948 T. V., and Aerts, R.: Carbon respiration from subsurface peat accelerated by climate  
949 warming in the sub- arctic, *Nature*, 460, 616-619, 2009.
- 950 Druel, A., Peylin, P., Krinner, G., Ciais, P., Viovy, N., Peregon, A., Barstrikov, V.,  
951 Kosykh, N., Mironycheva-Tokareva, N.: Towards a more detailed representation of  
952 high-latitude vegetation in the global land surface model ORCHIDEE (ORC-HL-  
953 VEGv1.0), *Geoscientific Model Development*, 10(12), 4693–4722,  
954 <https://doi.org/10.5194/gmd-10-4693-2017>, 2017.
- 955 Duarte, H. F., Raczka, B. M., Ricciuto, D. M., Lin, J. C., Koven, C. D., Thornton, P. E.,  
956 Bowling, D. R., Lai, C. T., Bible, K. J. and Ehleringer, J. R.: Evaluating the  
957 Community Land Model (CLM4.5) at a coniferous forest site in northwestern United  
958 States using flux and carbon-isotope measurements, *Biogeosciences*, 14(18): 4315-  
959 4340, DOI: 10.5194/bg-14-4315-2017, 2017.
- 960 Euskirchen, E.S., McGuire, A.D., Chapin, F.S. III, Yi, S., and Thompson, C.C.: Changes  
961 in vegetation in northern Alaska under scenarios of climate change, 2003–2100:  
962 implications for climate feedbacks, *Ecological Applications* 19: 1022-1043, 2009.
- 963 Farquhar, G.D., von Caemmerer, S. and Berry, J.A.: A biochemical model of  
964 photosynthetic CO<sub>2</sub> assimilation in leaves of C<sub>3</sub> species. *Planta*, 149, 78-90, 1980.
- 965 Fenner, N., Ostle, N.J., Mcnamara, N., Sparks, T., Harmens, H., Reynolds, B., and  
966 Freeman, C.: Elevated CO<sub>2</sub> effects on peat- land plant community carbon dynamics  
967 and DOC production, *Ecosystem*, 10,635-647,2007.
- 968 Frohking, S. and Roulet, N.T.: Holocene radiative forcing impact of northern peatland  
969 carbon accumulation and methane emissions, *Glob. Change Biol.* 13, 1079-1088,  
970 2007.
- 971  
972 Girardin, M. P., Bouriaud, O., Hogg, E. H., Kurz, W., Zimmermann, N. E., Metsaranta, J.  
973 M., Jong, Rogier de, Frank, D. C., Esper, J., Büntgen, U., Guo, X., and Bhatti, J.: No  
974 growth stimulation of Canada’s boreal forest under half-century of combined warming  
975 and CO<sub>2</sub> fertilization, *Proceedings of the National Academy of Science*, 113(52),  
976 E8406–E8414, 2016.
- 977 Goetz, J.D., and Price, J.S.: Role of morphological structure and layering of Sphagnum  
978 and Tomenthypnum mosses on moss productivity and evaporation rates, *Canadian*  
979 *Journal of Soil Sciences*. DOI:10.4141/ CJSS-2014-092, 2015.

- 980 Golaz, J.-C., Caldwell, P. M., Van Roekel, L. P., Petersen, M. R., Tang, Q., Wolfe, J. D.,  
981 Abeshu, G., Anantharaj, V., Asay-Davis, X. S., Bader, D.C., Baldwin, S. A., Bisht, G.,  
982 Bogenschütz, P. A., Branstetter, M., Brunke, M., A., Brus, S.R., Burrows, S.M.,  
983 Cameron-Smith P. J., Donahue, A. S., Deakin, M., Easter, R. C., Evans, K. J., Feng,  
984 Y., Flanner, M., Foucar, J., G., Fyke, J. G., Griffin, B. M., Hannay, C., Harrop, B. E.,  
985 Hoffman, M. J., Hunke, E. C., Jacob, R. L., Jacobsen, D. W., Jeffery, N., Jones, P. W.,  
986 Klein, S. A., Larson, V. E., Leung, L. R., Li, H., Lin, W., Lipscomb, W.H., Ma, P.-L.,  
987 Mahajan, S., Maltrud, M., E., Mametjanov, A., McClean, J. L., McCoy, R. B., Neale,  
988 R.B., Price, S. F., Qian, Y., Rasch, P. J., Reeves Eyre, J.E.J., Riley, W. J., Ringler, T.  
989 D., Roberts, A. F., Roesler, E. L., Salinger, A. G., Shaheen, Z., Shi, X., Singh, B.,  
990 Tang, J., Taylor, M. A., Thornton, P. E., Tuner, A. K., Veneziani, M., Wan, H., Wang,  
991 H., Wang, S., Williams, D. N., Wolfram, P. J., Worley, P. H., Xie, S., Yang, Y., Yoon,  
992 J.-H., Zelinka, M. D., Zender, C. S., Zeng, X., Zhang, C., Zhang, K., Zhang, Y.,  
993 Zheng, X., Zhou, T., Zhu, Q.: The DOE E3SM coupled model version 1: Overview  
994 and evaluation at standard resolution, *J. Adv. Model Earth Sy*, 11(7), 2089-2129,  
995 <https://doi.org/10.1029/2018MS001603>, 2019.
- 996 Gong, J., Roulet, N., Froking, S., Peltola, H., Laine, A.M., Kokkonen, N., and Tuittila,  
997 E.-S.: Modelling the habitat preference of two key sphagnum species in a poor fen as  
998 controlled by capitulum water retention, *Biogeosciences Discussions*,  
999 <https://doi.org/10.5194/bg-2019-366>, 2019.
- 1000 Gorham, E.: Northern peatlands: role in the carbon cycle and probable responses to  
1001 climatic warming, *Ecological Applications*, 1, 182-195, 1991.
- 1002 Grant, R. F., Desai, A. R., and Sulman, B. N.: Modelling contrasting responses of  
1003 wetland productivity to changes in water table depth, *Biogeosciences*, 9, 4215-4231,  
1004 2012.
- 1005 Granath, G., Limpens, J., Posch, M., Muecher, S., and De Vries, W.: Spatio-temporal  
1006 trends of nitrogen deposition and climate effects on Sphagnum productivity in  
1007 European peatlands, *Environmental Pollution*, 187, 73-80, [https://doi.org/10.1016/j.](https://doi.org/10.1016/j.envpol.2013.12.023)  
1008 [envpol.2013.12.023](https://doi.org/10.1016/j.envpol.2013.12.023), 2014  
1009 Griffiths, N. A., and Sebestyen, S. D.: Dynamic vertical  
1010 profiles of peat porewater chemistry in a northern peatland, *Wetlands*, 36(6), 1119-  
1130, 2016.
- 1011 Griffiths, N. A., and Sebestyen, S. D.: Dynamic vertical profiles of peat porewater  
1012 chemistry in a northern peatland, *Wetland*, 36, 1119-1130, doi:10.1007/s13157-016-  
1013 0829-5, 2016.
- 1014 Griffiths, N. A., Hanson, P. J., Ricciuto, Iversen, C. M., Jensen, A.M., Malhotra, A.,  
1015 McFarlane, K. J., Norby, R. J., Sargsyan, K., Sebestyen, S. D., Shi, X., Walker, A. P.,  
1016 Ward, E. J., Warren, J. M., and Weston, D. J.: Temporal and spatial variation in  
1017 peatland carbon cycling and implications for interpreting responses of an ecosystem-  
1018 scale warming experiment, *Soil Sci. Soc. Am. J.*, 81(6), 1668-1688,  
1019 doi:10.2136/sssaj2016.12.0422, 2018.
- 1020 Grosvernier, P., Matthey, Y., and Buttler, A.: Growth potential of three Sphagnum  
1021 species in relation to water table level and peat properties with implications for their  
1022 restoration in cut-over bogs, *Journal of Applied Ecology*, 34(2), 471-483.  
1023 <https://doi.org/10.2307/2404891>, 1997.

- 1024 Grosvernier, P.R., Mitchell, E.A.D., Buttler, A., Gobat, J.M.: Effects of elevated CO<sub>2</sub> and  
 1025 nitrogen deposition on natural regeneration processes of cut-over ombrotrophic peat  
 1026 bogs in the Swiss Jura mountains, *Glob Change Prot Areas* 9, 347 – 35, 2001.
- 1027 Gundale, M.J., DeLuca, T.H., and Nordin, A.: Bryophytes attenuate anthropogenic  
 1028 nitrogen inputs in boreal forests, *Glob. Change Biol.*,17, 2743-2753, 2011.
- 1029 Gunnarsson, U., Granberg, G., & Nilsson, M.: Growth, production and interspecific  
 1030 competition in *Sphagnum*: effects of temperature, nitrogen and sulphur treatments on a  
 1031 boreal mire, *New Phytologist*, 163(2), 349-359, [https://doi.org/10.1111/j.1469-](https://doi.org/10.1111/j.1469-8137.2004.01108.x)  
 1032 [8137.2004.01108.x](https://doi.org/10.1111/j.1469-8137.2004.01108.x), 2004.
- 1033 Hanson, P. J., Riggs, J.S., Nettles, W. R., Krassovski, M. B., and Hook L. A.: SPRUCE  
 1034 deep peat heating (DPH) environmental data, February 2014 through July 2015, Oak  
 1035 Ridge National Laboratory, TES SFA, U.S. Department of Energy, Oak Ridge,  
 1036 Tennessee, U.S.A. <https://doi.org/10.3334/CDIAC/spruce.013>, 2015a.
- 1037 Hanson, P.J., Riggs, J.S. Dorrance, C., Nettles, W.R., and Hook, L.A.: SPRUCE  
 1038 Environmental Monitoring Data: 2010-2016. Carbon Dioxide Information Analysis  
 1039 Center, Oak Ridge National Laboratory, U.S. Department of Energy, Oak Ridge,  
 1040 Tennessee, U.S.A. <http://dx.doi.org/10.3334/CDIAC/spruce.001>, 2015b.
- 1041 Hanson, P. J., Riggs, J.S., Nettles, W.R., Phillips, J.R., Krassovski, M.B., Hook, L.A.,  
 1042 Gu, L., Richardson, A.D., Aubrecht, D.M., Ricciuto, D.M., Warren, J.M., and Barbier,  
 1043 C.: Attaining whole-ecosystem warming using air and deep-soil heating methods with  
 1044 an elevated CO<sub>2</sub> atmosphere, *Biogeosciences*, 14, 861-883, 2017.
- 1045  
 1046 Hanson, P.J., Phillips, J.R., Wullschelger, S. D., Nettles, W. R., Warren, J. M., Ward, E.  
 1047 J.: SPRUCE Tree Growth Assessments of *Picea* and *Larix* in S1-Bog Plots and  
 1048 SPRUCE Experimental Plots beginning in 2011, Oak Ridge National Laboratory, TES  
 1049 SFA, U.S. Department of Energy, Oak Ridge, Tennessee,  
 1050 U.S.A. <https://doi.org/10.25581/spruce.051/1433836>, 2018a.
- 1051  
 1052 Hanson, P.J., Phillips, J.R., Brice, D.J., and Hook, L.A.: SPRUCE Shrub-Layer Growth  
 1053 Assessments in S1-Bog Plots and SPRUCE Experimental Plots beginning in  
 1054 2010. Oak Ridge National Laboratory, TES SFA, U.S. Department of Energy, Oak  
 1055 Ridge, Tennessee, U.S.A. <https://doi.org/10.25581/spruce.052/1433837>, 2018b.
- 1056 Hanson, P. J., Griffiths, N.A., Iversen, C.M., Norby, R. J., Sebestyen, S. D., Phillips,  
 1057 Jeffrey, J. R., Chanton, P., Kolka, R. K., Malhotra, A., Oleheiser, K. C., Warren, J. M.,  
 1058 Shi, X., Yang, X., Mao, J., and Ricciuto, D., M.: Rapid net carbon loss from a whole-  
 1059 ecosystem warmed peatland. *AGU Advances*, 1, e2020AV000163,  
 1060 <https://doi.org/10.1029/2020AV000163>, 2020.
- 1061 Heijmans, M., Arp, W.J., Berendse, F.: Effects of elevated CO<sub>2</sub> and vascular plants on  
 1062 evapotranspiration in bog vegetation, *Glob Change Biol* 7:817 – 827, 2001.

- 1063 Heijmans, M.M.P.D., Arp, W.J., and Chapin, F.S. III.: Carbon dioxide and water vapour  
 1064 exchange from understory species in boreal forest, *Agricultural and Forest*  
 1065 *Meteorology* 123,135-147, DOI:10.1016/j. agrformet.2003.12.006, 2004a.
- 1066 Heijmans, M.M.P.D, Arp, W.J., and Chapin, F.S. III.: Controls on moss evaporation in a  
 1067 boreal black spruce forest. *Global Biogeochemical Cycles* 18(2), 1-8,  
 1068 DOI:10.1029/2003GB002128, 2004b.
- 1069 Heijmans, M.M. P. D., Mauquoy, D., van Geel, B., and Berendse, F.: Long-term effects  
 1070 of climate change on vegetation and carbon dynamics in peat bogs. *Journal of*  
 1071 *Vegetation Science* 19, 307-320, 2008.
- 1072 Hobbie, S.E., and Chapin, F.S. III.: The response of tundra plant biomass, aboveground  
 1073 production, nitrogen, and CO<sub>2</sub> flux to experimental warming, *Ecology*, 79,1526-1544,  
 1074 1998.
- 1075 Hobbie, S.E., Shevtsova, A., and Chapin, F.S.III.: Plant responses to species removal and  
 1076 experimental warming in Alaskan Tus- sock Tundra. *Oikos* 84,417-434, 1999.
- 1077 Hoosbeek, M.R., Van Breemen, N., Vasander, H., Buttler, A., Berendse, F.: Potassium  
 1078 limits potential growth of bog vegetation under elevated atmospheric CO<sub>2</sub> and N  
 1079 deposition, *Glob. Change Biol.*, 8,1130-1138, [https://doi.org/10.1046/j.1365-](https://doi.org/10.1046/j.1365-2486.2002.00535.x)  
 1080 [2486.2002.00535.x](https://doi.org/10.1046/j.1365-2486.2002.00535.x), 2002.
- 1081 Ise, T., Dunn, A. L., Wofsy, S. C., and Moorcroft, P. R.: High sensitivity of peat  
 1082 decomposition to climate change through water table feedback, *Nat. Geosci.*, 1, 763-  
 1083 766, 2008.
- 1084 Jauhiainen, J., Silvola, J.: Photosynthesis of *Sphagnum fuscum* at long-term raised CO<sub>2</sub>  
 1085 concentrations, *Annales Botanici Fennici*, 36,11-19, 1999.
- 1086 Jensen, A.M., Warren, J. M., Hook, L. A., Wullschleger, S. D., Brice, D.J., Childs, J.,  
 1087 and Vander Stel, H.M.: SPRUCE S1 Bog Pretreatment Seasonal Photosynthesis and  
 1088 Respiration of Trees, Shrubs, and Herbaceous Plants, 2010-2015, Oak Ridge National  
 1089 Laboratory, TES SFA, U.S. Department of Energy, Oak Ridge, Tennessee, U.S.A.,  
 1090 <https://doi.org/10.3334/CDIAC/spruce.008>, 2018.
- 1091 Jensen, A.M., Warren, J. M., King, A., Ricciuto, D.M., Hanson, P. J., and Wullschleger,  
 1092 S. D.: Simulated projections of boreal forest peatland ecosystem productivity are  
 1093 sensitive to observed seasonality in leaf phenology, *Tree Physiology*, 39(4), 556-572,  
 1094 doi: 10.1093/treephys/tpy140, 2019.
- 1095 Jiang, J., Huang, Y., Ma, S., Stacy, M., Shi, Z., Ricciuto, D. M., Hanson, P. J., and Luo,  
 1096 Y.: Forecasting Responses of a Northern Peatland Carbon Cycle to Elevated CO<sub>2</sub> and  
 1097 a Gradient of Experimental Warming, *J. Geophys. Res.-Biogeo*, 123(3), 1057-1071,  
 1098 doi: 10.1002/2017JG004040, 2018.

- 1099 Juday, G. P., and Alix, C.: Consistent negative temperature sensitivity and positive  
 1100 influence of precipitation on growth of floodplain *Picea glauca* in Interior Alaska,  
 1101 *Canadian Journal of Forest Research*, 42, 561-573, 2012.  
 1102
- 1103 Kostka, J.E., Weston, D.J., Glass, J.B., Lilleskov, E.A., Shaw, A.J., and Turetsky, M.R.:  
 1104 The Sphagnum microbiome: new insights from an ancient plant lineage, *New*  
 1105 *Phytologist*, 211(1):57-64, 2016
- 1106 Kuiper, J. J., Mooij, W. M., Bragazza, L., and Robroek, B. J.: Plant functional types  
 1107 define magnitude of drought response in peatland CO<sub>2</sub> exchange, *Ecology*, 95, 123-  
 1108 131, <https://doi.org/10.1890/13-0270.1>, 2014.
- 1109 Lafleur, P. M., Hember, R. A., Admiral, S. W., and Roulet, N. T.: Annual and seasonal  
 1110 variability in evapotranspiration and water table at a shrub-covered bog in southern  
 1111 Ontario, Canada, *Hydrol. Process.*, 19, 3533–3550, <https://doi.org/10.1002/hyp.5842>,  
 1112 2005.
- 1113 Larmola, T., Leppänen, S. M., Tuittila, E.-Stiina, Aarva, M., Merilä, P., Fritze, H.,  
 1114 Tiirola, M.: Methanotrophy induces nitrogen fixation during peatland development,  
 1115 *PNAS*, 734-739, [www.pnas.org/cgi/dio/10.1073/pnas.1314284111](http://www.pnas.org/cgi/dio/10.1073/pnas.1314284111), 2014.
- 1116 Launiainen, S., Katul, G. G., Lauren, A., and Kolari, P.: Coupling boreal forest CO<sub>2</sub>, H<sub>2</sub>O  
 1117 and energy flow by a vertically structured forest canopy-Soil model with separate  
 1118 bryophyte layer. *Ecological Modelling*, 312, 385-405.  
 1119 <https://doi.org/10.1016/j.ecolmodel.2015.06.007>, 2015.
- 1120 Lindo, Z, and Gonzalez, A.: The bryosphere: an integral and influential component of the  
 1121 earth's biosphere, *Ecosystems*, 13, 612–627, 2010.
- 1122 Lindo, Z., Nilsson, M.C., and Gundale, M.J.: Bryophyte-cyanobacteria associations as  
 1123 regulators of the northern latitude carbon balance in response to global change, *Glob.*  
 1124 *Change Biol.*, 19(7),2022-35, 2013.
- 1125 Lu, D., Ricciuto, D.M., Stoyanov, M., and Gu, L.: Calibration of the E3SM Land Model  
 1126 Using Surrogate-Based Global Optimization, *J Adv Model Earth Sy*, 10(6), 1337-  
 1127 1356, doi: 10.1002/2017ms001134, 2018.
- 1128 Lu, D., and Ricciuto, D.M.: Efficient surrogate modeling methods for large-scale Earth  
 1129 system models based on machine-learning techniques, *Geosci Model Dev*, 12(5),  
 1130 1791-1807, doi: 10.5194/gmd-12-1791-2019, 2019.
- 1131 Man, R., Kayahara, G.J., Rice, J.A., and MacDonald, G.B.: Eleven- year responses of a  
 1132 boreal mixedwood stand to partial harvesting: light, vegetation, and regeneration  
 1133 dynamics, *For Ecol Manag* 255,697-706, 2008.

- 1134 Mazziotta, A., Granath, G., Rydin, H. and Bengtsson F.: Scaling functional traits to  
 1135 ecosystem processes: Towards a mechanistic understanding in peat mosses, *Journal of*  
 1136 *Ecology*, DOI:10.1111/1365-2745.13110, 2018.
- 1137 Metcalfe, D. B., Ricciuto D. M., Palmroth, S., Campbell, Hurry, C., V., Mao, J., Keel, S.  
 1138 G., Linder, S., Shi, X., Näsholm, T., Ohlsson, K. E. A., Blackburn, M., Thornton, P. E.  
 1139 and Oren, R.: Informing climate models with rapid chamber measurements of forest  
 1140 carbon uptake, *Global Change Biology*, 23(5), 2130-2139, DOI: 10.1111/gcb.13451,  
 1141 2017.
- 1142 McFadden, J.P., Eugster, W., Chapin, F.S.III.: A regional study of the controls on water  
 1143 vapor and CO<sub>2</sub> exchange in Arctic tundra, *Ecology*, 84,2762-76, 2003.
- 1144 McGuire, A. D., Anderson, L. G., Christensen, T. R., Dallimore, S., Guo, L., Hayes, D.  
 1145 J., Heimann, M., Lorenson, T. D., Macdonald, R. W. and Roulet, N.: Sensitivity of the  
 1146 carbon cycle in the Arctic to climate change, *Ecol. Monogr.*, 79, 523-555, 2009.
- 1147 McPartland, M. Y., Montgomery, R. A., Hanson, P. J., Phillips, J. R., Kolka, R., Palik B.:  
 1148 Vascular plant species response to warming and elevated carbon dioxide in a boreal  
 1149 peatland, *Environ. Res. Lett.*, <https://doi.org/10.1088/1748-9236/abc4fb>, 2020.
- 1150 Miller, P. A. and Smith, B.: Modelling Tundra Vegetation Response to Recent Arctic  
 1151 Warming, *Ambio*, 41, 281-291, <https://doi.org/10.1007/s13280-012-0306-1>, 2012.
- 1152 Mokhov, I.I., Eliseev, A.V., and Denisov, S.N.: Model diagnostics of variations in  
 1153 methane emissions by wetlands in the second half of the 20th century based on  
 1154 reanalysis data, *Dokl. Earth Sci.*, 417(1),1293-1297, 2007.
- 1155 Moore, T.R., Roulet, N.T., and Waddington, J.M.: Uncertainty in predicting the effect of  
 1156 climate change on the carbon cycling of Canadian peatlands, *Clim. Change*, 40, 229-  
 1157 245, 1998.
- 1158 Myneni, R. B., Keeling, C. D., Tucker, C. J., Asrar, G., and Nemani, R. R.: Increased  
 1159 plant growth in the northern high latitudes from 1981 to 199,1 *Nature*, 386,698-702,  
 1160 1997.
- 1161 Murray, K.J., Tenhunen, J.D., and Nowak, R.S.: Photoinhibition as a control on  
 1162 photosynthesis and production of Sphagnum mosses, *Oecologia*, 96,200-207, 1993.
- 1163 Nichols, J.E., and Peteet, D.M.: Rapid expansion of northern peatlands and doubled  
 1164 estimate of carbon storage, *Nat. Geosci.* 12, 917-921, doi:10.1038/s41561-019-0454-z,  
 1165 2019.
- 1166 Nilsson, M.C., and Wardle, D.A.: Understory vegetation as a forest ecosystem driver:  
 1167 evidence from the northern Swedish boreal forest, *Frontiers in Ecology and the*  
 1168 *Environment*, 3, 421-428, 2005.
- 1169 Norby, R.J., and Childs, J.: Sphagnum productivity and community composition  
 1170 in the SPRUCE experimental plots. *Carbon Dioxide Information Analysis*



- 1171 Center, Oak Ridge National Laboratory, U.S. Department of Energy, Oak  
1172 Ridge, Tennessee, U.S.A. <http://dx.doi.org/10.3334/CDIAC/spruce.xxx>, 2017.
- 1173 Norby, R.J., Childs, J., Hanson, P.J., and Warren, J.M.: Rapid loss of an ecosystem  
1174 engineer: Sphagnum decline in an experimentally warmed bog, *Ecology and*  
1175 *Evolution*, 9(22), 12571-12585, <https://doi.org/10.1002/ece3.5722>, 2019.
- 1176 Nungesser, M. K.: Modelling microtopography in boreal peatlands: Hummocks and  
1177 hollows, *Ecol. Model.*, 165(2-3), 175-207, 2003.
- 1178
- 1179 Oechel, W.C., and Van Cleve, K.: The role of bryophytes in nutrient cycling in the taiga,  
1180 in *Ecological Studies*, Vol. 57: Forest Ecosystems in the Alaskan Taiga, edited by:  
1181 Van Cleve, K., Chapin III, F. S., Flanagan, P.W., Viereck, L.A., and Dyrness, C.T.,  
1182 Springer-Verlag, New York, 121-137, 1986.
- 1183 Oleson, K. W., Lawrence, D. W., Bonan, G. B., Drewniak, B., Huang, M., Koven, C. D.,  
1184 Levis, S., Li, F., Riley, W. J., Subin, Z. M., Swenson, S. C., Thornton, P. E., Bozbiyik,  
1185 A., Fisher, R., Heald, C. L., Kluzek, E., Lamarque, J., Lawrence, P. J., Leung, L. R.,  
1186 Lipscomb, W., Muszala, S., Ricciuto, D. M., Sacks, W., Sun, Y., Tang, J., and Yang,  
1187 Z.: Technical description of version 4.5 of the Community Land Model (CLM),  
1188 NCAR/TN-503+STR, NCAR Technical Note, 2013.
- 1189 Park, H., Launiainen, S., Konstantinov, P. Y., Iijima, Y., and Fedorov, A. N.: Modeling  
1190 the effect of moss cover on soil temperature and carbon fluxes at a tundra site in  
1191 northeastern Siberia, *J. Geophys. Res.-Bioge*, 123, 3028-3044, [https://doi.org/](https://doi.org/10.1029/2018JG004491)  
1192 [10.1029/2018JG004491](https://doi.org/10.1029/2018JG004491), 2018.
- 1193 Parsekian, A. D., Slater, L., Ntarlagiannis, D., Nolan, J., S. Sebestyen, D., Kolka, R. K.,  
1194 and Hanson, P. J.: Uncertainty in peat volume and soil carbon estimated using ground-  
1195 penetrating radar and probing. *Soil Sci. Soc. Am. J.*, 76, 1911-1918. DOI:  
1196 [10.2136/sssaj2012.0040](https://doi.org/10.2136/sssaj2012.0040), 2012.
- 1197 Pastor, J., Peckham, B., Bridgman, S., Weltzin, J., and Chen, J.: Plant community  
1198 dynamics, nutrient cycling, and alternative stable equilibria in peatlands, *The*  
1199 *American Naturalist* 160, 553-568, 2002.
- 1200 Petrone, R., Solondz, D., Macrae, M., Gignac, D., and Devito, K.J.: Microtopographical  
1201 and canopy cover controls on moss carbon dioxide exchange in a western boreal plain  
1202 peatland, *Ecohydrology*, 4, 115-129, 2011.
- 1203 Porada, P., Weber, B., Elbert, W., Pöschl, U., and Kleidon, A.: Estimating global carbon  
1204 uptake by lichens and bryophytes with a process-based model, *Biogeosciences*, 10,  
1205 6989–7033, doi:10.5194/bg-10-6989-2013, 2013.
- 1206 Porada, P., Ekici, A., and Beer, C.: Effects of bryophyte and lichen cover on permafrost  
1207 soil temperature at large scale, *The Cryosphere*, 10(5), 2291–2315,  
1208 <https://doi.org/10.5194/tc-10-2291-2016>, 2016.

- 1209 Raczka, B., Duarte, H. F., Koven, C. D., Ricciuto, D.M., Thornton, P. E., Lin, J. C. and  
 1210 Bowling, D. R.: An observational constraint on stomatal function in forests: evaluating  
 1211 coupled carbon and water vapor exchange with carbon isotopes in the Community  
 1212 Land Model (CLM4.5), *Biogeosciences*, 13(18), 5183-5204, DOI: 10.5194/bg-13-  
 1213 5183-2016, 2016.
- 1214 Raghoebarsing, A. A., Smolders, A.J.P., Schmid, M.C., Rijpstra, W.I.C., Wolters-Arts,  
 1215 M., Derksen, J., Jetten, M.S.M., Schouten, S., Sinninghe Damsté, J.S., Lamers,  
 1216 L.P.M., Roelofs, J.G.M., Op den Camp, H.J.M., and Strous, M.: Methanotrophic  
 1217 symbionts provide carbon for photosynthesis in peat bogs. *Nature*, 436, 1153-1156,  
 1218 doi:10.1038/nature03802, 2005.
- 1219
- 1220 Ricciuto, D. M., Sargsyan, K., and Thornton, P.E.: The Impact of Parametric  
 1221 Uncertainties on Biogeochemistry in the E3SM Land Model, *J Adv Model Earth Sy*,  
 1222 10(2), 297-319, doi: 10.1002/2017ms000962, 2018.
- 1223 Ricciuto, D.M., Xu, X., Shi, X., Wang, Y., Song, X., Schadt, C.W., Griffiths, N. A., Mao,  
 1224 J., Warre, J.,M., Thornton, P.E., Chanton, J., Keller, J., Bridgham, S., Gutknecht, J.,  
 1225 Sebestyen, S. D., Finzi, A., Kolka, R., and Hanson P.J.: An Integrative Model for Soil  
 1226 Biogeochemistry and Methane Processes: I. Model Structure and Sensitivity Analysis,  
 1227 *J. Geophys. Res.-Biogeo*, In review, 2019.
- 1228 Riutta, T., Laine, J., and Tuittila, E.-S.: Sensitivity of CO<sub>2</sub> exchange of fen ecosystem  
 1229 componetns to water level variation, *Ecosystem*, 10(5), 718-733, 2007.
- 1230 Robroek, B.J.M., Limpens, J., Breeuwer, A., and Schouten, M.G.C.: Effects of water  
 1231 level and temperature on performance of four Sphagnum mosses. *Plant*  
 1232 *Ecology*, 190, 97-107, 2007.
- 1233 Robroek, B.J.M., Schouten, M.G.C., Limpens, J., Berendse F. and Poorter, H.: Interactive  
 1234 effects of water table and precipitation on net CO<sub>2</sub> assimilation of three co-occurring  
 1235 Sphagnum mosses differing in distribution above the water table, *Glob. Change Biol.*,  
 1236 15, 680-691, 2009.
- 1237 Rosenzweig, C., Karoly, D., Vicarelli, M., Neofotis, P., Wu, Q., Casassa, G., Menzel, A.,  
 1238 Root, T., Estrella, N., Seguin, B., Tryjanowski, P., Liu, C., Ravlins, S., and Imeson,  
 1239 A.: Attributing physical and biological impacts to anthropogenic climate  
 1240 change, *Nature*, 453, 353-357, doi:10.1038/nature06937, 2008.
- 1241 Rydin, H.: Effect of water level on desiccation of Sphagnum in relation to surrounding  
 1242 Sphagna, *Oikos*, 45(3), 374-379, <https://doi:10.2307/3565573>, 1985.
- 1243 Rydin, H., and Clymo, R. S.: Transport of carbon and phosphorus-compounds about  
 1244 Sphagnum. *Proceedings of the Royal Society Series B-Biological Sciences*,  
 1245 237(1286), 63-84, <https://doi:10.1098/rspb.1989.0037>, 1989.
- 1246 Rousk, K., Rousk, J., Jones, D.L., Zackrisson, O., DeLuca, and T.H.: Feather moss  
 1247 nitrogen acquisition across natural fertility gradients in boreal forests, *Soil Biol*  
 1248 *Biochem*, 61, 86-95, 2013.

- 1249 Rousk, K., and Michelsen, A.: The sensitivity of Moss-Associated Nitrogen Fixtion  
1250 towards Repeated Nitrogen Input, *Plos One*, 11(1), e0146655,  
1251 <https://doi.org/10.1371/journal.pone.0146655>, 2016.
- 1252 Rydsaa, J. H., Stordal, F., Bryn, A., and Tallaksen, L. M.: Effects of shrub and tree cover  
1253 increase on the near-surface atmosphere in northern Fennoscandia, *Biogeosciences*,  
1254 14, 4209-4227, <https://doi.org/10.5194/bg-14-4209-2017>, 2017.
- 1255 Saarnio, S., Jarvio, S., Saarinen, T., Vasander, H., Silvola, J.: Minor changes in  
1256 vegetation and carbon gas balance in a boreal mire under a raised CO<sub>2</sub> or NH<sub>4</sub>NO<sub>3</sub>  
1257 supply, *Ecosystems* 6:46-60, <https://doi.org/10.1007/s10021-002-0208-3>, 2003.
- 1258 Sargsyan, K., Safta, C., Najm, H. N., Debusschere, B. J., Ricciuto, D.M., and Thornton,  
1259 P.E.: Dimensionality Reduction for Complex Models Via Bayesian Compressive  
1260 Sensing, *International Journal for Uncertainty Quantification*, 4(1), 63-93, doi:  
1261 10.1615/Int.J.UncertaintyQuantification.2013006821, 2014.
- 1262 Sebestyen, S. D., Dorrance, C., Olson, D. M., Verry, E. S., Kolka, R. K., Elling, A. E.,  
1263 and Kyllander, R.: Long-term monitoring sites and trends at the Marcell Experimental  
1264 Forest, in: *Peatland biogeochemistry and watershed hydrology at the Marcell*  
1265 *Experimental Forest*, edited by: Kolka, R. K. Sebestyen, S. D., Verry, E. S., and  
1266 Brooks, CRC Press, New York, 15-71, 2011.
- 1267 Shi, X., Thornton, P. E., Ricciuto, D. M., Hanson, P. J., Mao, J., Sebestyen, S. D.,  
1268 Griffiths, N. A., and Bisht, G.: Representing northern peatland microtopography and  
1269 hydrology within the Community Land Model, *Biogeosciences*, 12(21), 6463-6477,  
1270 <https://doi.org/10.5194/bg-12-6463-2015>, 2015.
- 1271 Silva, L. C. R., Anand, M., and Leithead, M. D.: Recent widespread tree growth decline  
1272 despite increasing atmospheric CO<sub>2</sub>, *PLoS ONE*, 5(7), e11543, doi:  
1273 10.1371/journal.pone.0011543, 2010.
- 1274
- 1275 Sonnentag, O., Van Der Kamp, G., Barr, A.G., and Chen, J.: on the relationship between  
1276 water table depth and water vapor and carbon dioxide fluxes in a minerotrophic fen,  
1277 *Glob. Change Biol.*, 16(6), 1761-1776, [https://doi.org/10.1111/j.1365-](https://doi.org/10.1111/j.1365-2486.2009.02032.x)  
1278 2486.2009.02032.x, 2010.
- 1279 St-Hilaire, F., Wu, J., Roulet, N. T., Frohling, S., Lafleur, P. M., Humphreys, E. R., and  
1280 Arora, V.: McGill wetland model: evaluation of a peatland carbon simulator  
1281 developed for global assessments, *Biogeosciences*, 7, 3517-3530, 2010.
- 1282 Tarnocai, C.: The effect of climate change on carbon in Canadian peatlands, *Glob Planet*  
1283 *Change*, 53, 4, 222-232, 2006.
- 1284 Tenhunen, J.D., Weber, J.A., Yocum, C.S. and Gates, D.M.: Development of a  
1285 photosynthesis model with an emphasis on ecological applications, *Oecologia*, 26,101-  
1286 119, 1976.
- 1287
- 1288 Tian, H., Lu,C., Yang, J., Banger, K., Huntinzger, D. N., Schwalm, C. R., Michalak, A.  
1289 M., Cook, R., Ciais, P., Hayes, D., Huang, M., Ito, A., Jacobson, A., Jain,A., Lei, H.,  
1290 Mao,J., Pan, S., Post, W.M, Peng, S., Poulter,B., Ren, W., Ricciuto,D.M., Schaefer, K.,  
1291 Shi, X., Tao,B., Wang, W., Wei, Y., Yang, Q., Zhang, B., and Zeng, N.: Global patterns

- 1292 of soil carbon stocks and fluxes as simulated by multiple terrestrial biosphere models:  
 1293 sources and magnitude uncertainty, *Global Biogeochem Cycles*, 29, 775-792,  
 1294 doi:10.1002/2014GB005021, 2015.
- 1295 Titus, J. E., Wagner, D.J., and Stephens, M.D.: Contrasting Water Relations of  
 1296 Photosynthesis for 2 Sphagnum Mosses, *Ecology*, 64, 1109-1115, 1983.
- 1297 Todd-Brown, K. E. O., Randerson, J. T., Post, W. M., Hoffman, F. M., Tarnocai, C.,  
 1298 Schuur, E. A. G., and Allison, S. D.: Causes of variation in soil carbon simulations  
 1299 from CMIP5 Earth system models and comparison with observations, *Biogeosciences*,  
 1300 10, 1717–1736, doi:10.5194/bg-10-1717-2013, 2013.
- 1301 Toet, S., Cornelissen, J.H., Aerts, R., van Logtestijn, R.S., de Beus, M., Stoevelaar, R.:  
 1302 Moss responses to elevated CO<sub>2</sub> and variation in hydrology in a temperate lowland  
 1303 peatland. *Plants and climate change*. Springer, Netherlands, pp 27-42, 2006.
- 1304 Turetsky, M. R., Wieder, R. K., and Vitt, D. H.: Boreal peatland C fluxes under varying  
 1305 permafrost regimes, *Soil Biol. Biochem.*,34,907-912, 2002.
- 1306 Turetsky, M. R., and Wieder, R. K.: Boreal bog Sphagnum refixes soil-produced and  
 1307 respired 14CO<sub>2</sub>, *Ecoscience*, 6(4), 587-591.  
 1308 <https://doi:10.1080/11956860.1999.11682559>, 1999.
- 1309 Turetsky, M.R., Mack, M.C., Hollingsworth, T.N., and Harden, J.W.: The role of mosses  
 1310 in ecosystem succession and function in Alaska’s boreal forest, *Canadian Journal of*  
 1311 *Forest Research* 4, 1237-1264, 2010.
- 1312 Turetsky, M. R., Bond-Lamberty, B., Euskirchen, E., Talbot, J., Frohling, S., McGuire,  
 1313 A. D., and Tuittila, E.-S.: The resilience and functional role of moss in boreal and arc-  
 1314 tic ecosystems, *New Phytol.*, 196, 49-67, doi:10.1111/j.1469- 8137.2012.04254.x,  
 1315 2012.
- 1316
- 1317 Van, B. N.: How Sphagnum bogs down other plants, *Trends Ecol. Evol*, 10, 270-275,  
 1318 1995.
- 1319 Van Der Heijden, E., Verbeek, S.K., Kuiper, P.J.C.: Elevated atmospheric CO<sub>2</sub> and  
 1320 increased nitrogen deposition: effects on C and N metabolism and growth of the peat  
 1321 moss *Sphagnum recurvum* P. Beauv. var. *mucronatum* (Russ.), *Warnst. Glob Change*  
 1322 *Biol* 6, 201 – 212, <https://doi.org/10.1046/j.1365-2486.2000.00303.x>, 2000.
- 1323 van der Schaaf, S.: Bog hydrology, in: *Conservation and Restoration of Raised Bogs:*  
 1324 *Geological, Hydrological and Ecological Studies*, edited by: Schouten, M.G.C., The  
 1325 Government Stationery Office, Dublin, 54-109, 2002.
- 1326 van der Wal, R., Pearce, I.S.K and Brooker, R.W.: Mosses and the struggle for light in a  
 1327 nitrogen-polluted world, *Oecologia*, 142,159-68, 2005.
- 1328 Van Gaalen, K. E., Flanagan, L. B., and Peddle, D. R.: Photosynthesis, chlorophyll  
 1329 fluorescence and spectral reflectance in Sphagnum moss at varying water contents,  
 1330 *Oecologia*, 153(1), 19-28, doi:10.1007/s00442-007-0718-y, 2007.

- 1331 Verry, E. S., and Janssens, J.: Geology, vegetation, and hydrology of the S2 bog at the  
 1332 MEF: 12,000 years in northern Minnesota, in *Peatland biogeochemistry and watershed*  
 1333 *hydrology at the Marcell Experimental Forest*, edited by R. K. Kolka S. D.  
 1334 Sebestyen, E. S. Verry, K.N. Brooks, CRC Press, New York, 93-134, 2011.
- 1335 Vile, M. A., Kelman Wieder, R., Živković, T., Scott, K. D., Vitt, D. H., Hartsock, J. A.,  
 1336 Iosue, C. L., Quinn, J.C., Petix, M., Fillingim, H.M., Popma, J.M.A., Dynarski, K.A.,  
 1337 Jackman, T. R., Albright, C.M., and Wykoff, D. D. : N<sub>2</sub>-fixation by methanotrophs  
 1338 sustains carbon and nitrogen accumulation in pristine peatlands, *Biogeochemistry*,  
 1339 121, 317-328, <https://doi.org/10.1007/s10533-014-0019-6>, 2014.
- 1340 Vitt, D. H.: A key and review of bryophytes common in North American peatlands,  
 1341 *Evansia*, 31, 121-158, 2014.
- 1342 Wania, R., Ross, I., Prentice, I.C.: Integrating peatlands and permafrost into a dynamic  
 1343 global vegetation model: 1. Evaluation and sensitivity of physical land surface  
 1344 processes, *Global Biogeochem. Cycles* 23, GB3014, doi:10.1029/2008GB003412,  
 1345 2009.
- 1346 Wania, R., Melton, J. R., Hodson, E. L., Poulter, B., Ringeval, B., Spahni, R., Bohn, T.,  
 1347 Avis, C. A., Chen, G., Eliseev, A. V., Hopcroft, P. O., Riley, W. J., Subin, Z. M., Tian,  
 1348 H., van Bodegom, P.M. , Kleinen, T. , Yu, Z., Singarayer, J. S., Zurcher, S.,  
 1349 Lettenmaier, D. P., Beerling, D. J., Denisov, S. N., Prigent, C., Papa, F., and Kaplan, J.  
 1350 O.: Present state of global wetland extent and wetland methane modelling:  
 1351 methodology of a model inter-comparison project (WETCHIMP), *Geosci. Model*  
 1352 *Dev.*, 6, 617-641, 2013.
- 1353 Walker, M.D., Wahren, C.H., Hollister, R.D., Henry, G.H.R., Ahlquist, L.E., Alatalo,  
 1354 J.M., Bret-Harte, M.S., Calef, M.P., Callaghan, T.V., Carroll, A.B., Epstein, H.E.,  
 1355 Jonsdottir, I.S., Klein, J.A., Magnusson, B., Molau, U., Oberbauer, S.F., Rewa, S.P.,  
 1356 Robinson, C.H., Shaver, G.R., Suding, K.N., Thompson, C.C., Tolvanen, A., Totland,  
 1357 O., Turner, P.L., Tweedie, C.E., Webber, and P.J., Wookey, P.A.: Plant community  
 1358 responses to experimental warming across the tundra biome, *Proc Natl Acad Sci USA*,  
 1359 10,31342-6, 2006.
- 1360 Walker, T. N., Ward, S. E., Ostle, N. J., and Bardgett, R. D.: Contrasting growth  
 1361 responses of dominant peatland plants to warming and vegetation composition,  
 1362 *Oecologia*, 178, 141-151, <https://doi.org/10.1007/s00442-015-3254-1>, 2015.
- 1363 Walker, A. P., Carter, K. R., Gu, L., Hanson, P. J., Malhotra, A., Norby, R.J., Sebestyen,  
 1364 S. D., Wullschlegel, S. D., Weston, D. J.: 2017. Biophysical drivers of seasonal  
 1365 variability in Sphagnum gross primary production in a northern temperate bog, *J.*  
 1366 *Geophys. Res.-Biogeo*, 122, 1078-1097, <https://doi.org/10.1002/2016JG003711>, 2017.
- 1367 Wang, H., Richardson, C. J., and Ho, M.: Dual controls on carbon loss during drought in  
 1368 peatlands, *Nature Climate Change*, 5, 58- 587, 2015.

- 1369 Ward, S. E., Ostle, N. J., Oakley, S., Quirk, H., Henrys, P. A., and Bardgett, R. D.:  
 1370 Warming effects on greenhouse gas fluxes in peatlands are modulated by vegetation  
 1371 composition, *Ecol. Lett.*, 16, 1285-1293, 2013.
- 1372 Weltzin, J. F., Harth, C., Bridgman, S. D., Pastor, J., and Vonderharr, M.: Production and  
 1373 microtopography of bog bryophytes: response to warming and water-table  
 1374 manipulations, *Oecologia*, 128(4), 557-565, [https://doi:10.1007/s004420100691](https://doi.org/10.1007/s004420100691), 2001.
- 1375 Weston, D.J., Timm, C.M., Walker, A.P., Gu, L., Muchero, W., Schmuta, J., Shaw, A. J.,  
 1376 Tuskan, G. A., Warren, J.M., and Willschleger, S.D.: Sphagnum physiology in the  
 1377 context of changing climate: Emergent influences of genomics, modeling and host-  
 1378 microbiome interactions on understanding ecosystem function, *Plant, Cell and*  
 1379 *Environment*, 38, 1737-1751, doi: 10.1111/pce.12458, 2015.
- 1380 White, M. A., Thornton, P. E., Running, S. W., and Nemani, R. R.: Parameterization and  
 1381 sensitivity analysis of the BIOME-BGC terrestrial ecosystem model: Net primary  
 1382 production controls, *Earth Interactions*, 4(3), 1-85, 2000.
- 1383 Wieder R. K.: Primary production in boreal peatlands. In: *Boreal peatland ecosystems*,  
 1384 edited by: Wieder, R. K., and Vitt, D. H., Springer-Verlag, Berlin Heidelberg,  
 1385 Germany, 145-163, 2006.
- 1386 Wiley, E., Rogers, B. J., Griesbauer, H. P., and Landhausser, S. M.: Spruce shows greater  
 1387 sensitivity to recent warming than Douglas-fir in central British Columbia, *Ecosphere*  
 1388 9(5), e02221, 10.1002/ecs2.2221, 2018 Williams T.G. and Flanagan, L.B.: Measuring  
 1389 and modelling environmental influences on photosynthetic gas exchange in Sphagnum  
 1390 and Pleurozium, *Plant Cell and Environment*, 21, 555-564, 1998.
- 1391 Williams T.G. & Flanagan L.B.: Measuring and modelling environmental influences on  
 1392 photosynthetic gas exchange in *Sphagnum* and Pleurozium, *Plant Cell and*  
 1393 *Environment*, 21, 555-564, 1998.
- 1394 Wilmking, M., Juday, G. P., Barber, V. A., and Zald, H. S. J.: Recent climate warming  
 1395 forces contrasting growth responses of white spruce at treeline in Alaska through  
 1396 temperature thresholds, *Glob. Change Biol.* 10, 1724-1736, 2004.
- 1397 Wolf, A., Callaghan, T. V., and Larson, K.: Future changes in vegetation and ecosystem  
 1398 function of the Barents Region, *Climatic Change*, 87, 51-73,  
 1399 <https://doi.org/10.1007/s10584-007-9342-4>, 2008.
- 1400 Wolken, J. M., Mann, D. H., Grant, T. A., Lloyd, A. H., Rupp, T.S., and Hollingsworth,  
 1401 T. N.: 2016. Climate-growth relationships along a black spruce to-pose-quence in  
 1402 interior Alaska, *Arctic, Antarctic, and Alpine Research*, 48, 637-652, 2016.
- 1403  
 1404 Wu, J., Roulet, N. T., Sagerfors, J., Nilsson, M. B.: Simulation of six years of carbon  
 1405 fluxes for a sedge-dominated oligotrophic minerogenic peatland in Northern Sweden  
 1406 using the McGill Wetland Model (MWM), *J. Geophys. Res. -Biogeosciences*,  
 1407 doi:10.1002/jgrg.20045, 2013.

- 1408 Wu, Y. and Blodau, C.: PEATBOG: a biogeochemical model for analyzing coupled  
1409 carbon and nitrogen dynamics in northern peatlands, *Geosci. Model Dev.*, 6, 1173-  
1410 1207, doi:10.5194/gmd-6-1173-2013, 2013.
- 1411 Wu, J. and Roulet, N. T.: Climate change reduces the capacity of northern peatlands to  
1412 absorb the atmospheric carbon dioxide: The different responses of bogs and fens,  
1413 *Global Biogeochem. Cycles*, doi.org/10.1002/2014GB004845, 2014.
- 1414 Wu, Y., Verseghy, D. L., and Melton, J. R.: Integrating peatlands into the coupled  
1415 Canadian Land Surface Scheme (CLASS) v3.6 and the Canadian Terrestrial  
1416 Ecosystem Model (CTEM) v2.0, *Geosci. Model Dev.*, 9, 2639-2663,  
1417 doi:10.5194/gmd-9-2639-2016, 2016.
- 1418 Yang, X., Ricciuto, D. M., Thornton, P. E., Shi, X., Xu, M., Hoffman, F., Norby R. J.:  
1419 The effects of phosphorus cycle dynamics on carbon sources and sinks in the Amazon  
1420 region: a modeling study using ELM v1, *J. Geophys. Res.-Biogeo*, 124,  
1421 <https://doi.org/10.1029/2019JG005082>, 2019.
- 1422 Yu, Z., Loisel, J., Brosseau, D. P., Beilman, D. W., and Hunt, S.J.: Global peatland  
1423 dynamics since the Last Glacial Maximum, *Geophys. Res. Lett.*, 37, L13402,  
1424 doi:10.1029/2010GL043584, 2010.
- 1425 Yurova, A., Wolf, A., Sagerfors, J., and Nilsson, M.: Variations in net ecosystem  
1426 exchange of carbon dioxide in a boreal mire: Modeling mechanisms linked to water  
1427 table position, *J. Geophys. Res.-Biogeo.*, 112, G02025, doi:10.1029/2006JG000342,  
1428 2007
- 1429 Zhang, W. X., Miller, P. A., Smith, B., Wania, R., Koenigk, T., and Doscher, R.: Tundra  
1430 shrubification and tree-line advance amplify arctic climate warming: results from an  
1431 individual- based dynamic vegetation model, *Environ. Res. Lett.*, 8, 034023,  
1432 <https://doi.org/10.1088/1748-9326/8/3/034023>, 2013.
- 1433 Zhuang, Q., Melillo, J.M., Sarofim, M.C., Kicklighter, D.W., McGuire, A.D., Felzer,  
1434 B.S., Sokolov, A., Prinn, R.G., Steudler, P.A., and Hu, S.: CO<sub>2</sub> and CH<sub>4</sub> exchanges  
1435 between land ecosystems and the atmosphere in northern high latitudes over the 21st  
1436 century, *Geophys. Res. Lett.*, 33, L17403, doi:10.1029/2006GL026972, 2006.  
1437  
1438